| | |
|---|---|
| Title | Differentiation of vascular stem cells contributes to ectopic calcification of atherosclerotic plaque |
| Author(s) | Leszczynska, Aleksandra; O'Doherty, Aideen; Farrell, Eric; Pindjakova, Jana; O'Brien, Fergal J.; O'Brien, Timothy; Barry, Frank; Murphy, Mary |
| Publication Date | 2016-02-27 |
| Publication Information | Leszczynska A;O'Doherty A;Farrell E;Pindjakova J;O'Brien FJ;O'Brien T;Barry F;Murphy M; (2016) 'Differentiation of Vascular Stem Cells Contributes to Ectopic Calcification of Atherosclerotic Plaque'. Stem Cells (Dayton, Ohio), 34 (4). |
| Publisher | Wiley |
| Link to publisher's version | http://dx.doi.org/10.1002/stem.2315 |
| Item record | http://hdl.handle.net/10379/5867 |
| DOI | http://dx.doi.org/10.1002/stem.2315 |

# Differentiation of Vascular Stem Cells Contributes to Ectopic Calcification of Atherosclerotic Plaque

Aleksandra Leszczynska, PhD[1, 2], Aideen O'Doherty, PhD[1], Eric Farrell, PhD[1, 3], Jana Pindjakova, PhD[1, 4], Fergal J. O'Brien, PhD[5], Timothy O'Brien, MD, PhD[1], Frank Barry, PhD[1], J. Mary Murphy, PhD[1]

[1]Regenerative Medicine Institute, National University of Ireland Galway, Galway, Ireland;
[2]Division of Cardiology, Johns Hopkins University School of Medicine, Baltimore, MD;
[3]The Department of Oral and Maxillofacial Surgery, Special Dental Care and Orthodontics, Erasmus MC, University Medical Centre, Rotterdam, the Netherlands;
[4]Integrated Center of Cellular Therapy and Regenerative Medicine, International Clinical Research Center, St. Anne's University Hospital, Brno, Czech Republic;
[5] Tissue Engineering Research Group, Department of Anatomy, Royal College of Surgeons in Ireland, Dublin, Ireland; Trinity Centre for Bioengineering, Trinity College Dublin, Dublin 2, Ireland; Advanced Materials and Bioengineering Research (AMBER) Centre, RCSI & TCD

**Corresponding Author:** Dr Mary Murphy, REMEDI, Biosciences Research, Dangan, National University of Ireland Galway, Galway, Ireland
Tel: +353 (0)91 495206; Fax: +353 (0)91 495547; E-mail: mary.murphy@nuigalway.ie

**Author Contributions:**

Aleksandra Leszczynska: Conception and design, Collection and/or assembly of data, Data analysis and interpretation, Manuscript writing, Final approval of manuscript

Aideen O'Doherty: Conception and design, Data analysis and interpretation, Final approval of manuscript

Eric Farrell: Provision of study material, Data analysis and interpretation, Manuscript writing, Final approval of manuscript

Jana Pindjakova: Data analysis and interpretation, Final approval of manuscript

Fergal O'Brien: Provision of study material or patients, Final approval of manuscript

Timothy O'Brien: Data analysis and interpretation, Final approval of manuscript

Frank Barry: Data analysis and interpretation, Final approval of manuscript

Mary Murphy: Conception and design, Data analysis and interpretation, Manuscript writing, Final approval of manuscript

**Abstract**

The cellular and molecular basis of vascular calcification (VC) in atherosclerosis is not fully understood. Here, we investigate role of resident/circulating progenitor cells in VC and contribution of inflammatory plaque environment to this process. VSCs and MSCs isolated from atherosclerotic ApoE$^{-/-}$ mice showed significantly more *in vitro* osteogenesis and chondrogenesis than cells generated from control C57BL/6 mice. To assess their ability to form bone *in vivo*, cells were primed chondrogenically or cultured in control medium on collagen glycosaminoglycan scaffolds *in vitro* prior to subcutaneous implantation in ApoE$^{-/-}$ and C57BL/6 mice using a crossover study design. Atherosclerotic ApoE$^{-/-}$ MSCs and VSCs formed bone when implanted in C57BL/6 mice. In ApoE$^{-/-}$ mice, these cells generated more mature bone than C57BL/6 cells. The atherosclerotic *in vivo* environment alone promoted bone formation by implanted C57BL/6 cells. Un-primed C57BL/6 VSCs were unable to form bone in either mouse strain. Treatment of ApoE$^{-/-}$ VSC chondrogenic cultures with interleukin (IL)-6 resulted in significantly increased glycosaminoglycan deposition and expression of characteristic chondrogenic genes at 21 days. In conclusion, resident vascular cells from atherosclerotic environment respond to the inflammatory milieu and undergo calcification. IL-6 may have a role in aberrant differentiation of VSCs contributing to vascular calcification in atherosclerosis.

**Keywords:** Mesenchymal stem cells, vascular progenitor cells, pericytes, atherosclerosis, vascular calcification, chondrogenesis, endochondral ossification, collagen scaffold, *in vivo*

**Nonstandard Abbreviations and Acronyms:**

| | |
|---|---|
| VSC | Vessel-derived stem/progenitor cells |
| MSC | Mesenchymal stem cells |
| SMC | Smooth muscle cells |
| BMMNC | Bone marrow mononuclear cell |
| EC | Endothelial cells |
| P/S | Penicillin/Streptomycin |
| P | Passage |
| GAG | Glycosaminoglycan |
| ACAN | Aggrecan |
| ALP | Alkaline phosphatase |
| RANKL | Receptor activator of nuclear factor-κB ligand |

## Introduction

Vasculature has a notably high capacity for repair throughout embryonic and adult life with the presence of a number of stem progenitor niches and/or lineages described [1, 2]. That progenitor cells, producing cells of vessel walls in the embryo, remain within their niche and become activated to repair/regenerate the vascular wall in adults is a topic of active interest [3, 4]. Progenitor cell populations such as hemangioblasts, circulating endothelial progenitor cells, smooth muscle progenitor cells, mesenchymal stem cells (MSC) and pericytes in vessel walls have been isolated and characterized [4-7]. The demonstrated multipotency of these cells has led to their association with vascular calcification (VC) in atherosclerosis. VC is an important complication of atherosclerosis contributing to cardiovascular morbidity and mortality [8], given the increased risk of heart attack with calcified coronaries and the growing incidence of calcified aortic stenosis [9]. It is increasingly accepted that VC is far from a passive degenerative process but an active, organized, complex and highly regulated process. In contrast to cardiac valvular and medial artery calcification, atherosclerotic-associated calcification is thought to occur by a process similar to endochondral ossification [10] with chondrocytes and osteoblasts detected in plaque [11]. In recent years, there has been growing interest in the role of resident progenitor cells as contributors to ectopic bone and cartilage formation. There is some evidence that resident vascular progenitor cells form nodules similar to calcified atherosclerotic plaques and get destabilized to factors like oxLDL akin to atherosclerotic plaques [12]. Moreover, similar to pericytes from other tissues, resident vascular pericytes have been shown to differentiate in aberrant tissues found in atherosclerotic plaque [13].

Here, we investigated the effect of the atherosclerotic environment on resident vessel-derived stem/progenitor cells (VSC) or bone marrow-derived MSC differentiation, representative of a circulating MSC population, in an attempt to elucidate their role in the formation of ectopic bone/cartilage in atherosclerotic plaque. The approach presented involved isolation and

characterization of VSCs and MSCs from aortae and marrow, respectively of normal, background C57BL/6 and atherosclerotic apolipoprotein E-null ($ApoE^{-/-}$) mice. Elements of plaque development such as early influx of inflammatory cytokines, formation of necrotic cores and accumulation of SMCs and fibrous tissue are similar to human disease in these mice [14]. The intrinsic capacity of the cell populations to form bone and the effect of the atherosclerotic host milieu on this process was assessed *in vivo*. Cells were loaded on a collagen-glycosaminoglycan scaffold [15] without priming or were first chondrogenically-primed *in vitro*. The effect of the atherosclerotic environment on bone formation was investigated by implanting both donor cell preparations into $ApoE^{-/-}$ recipient mice with constructs implanted in C57BL/6 mice as controls. The incidence, extent and quality of calcified cartilage and bone formation were assessed by a histological grading system.

In an attempt to understand the mechanism of ectopic vascular bone formation, the effect of pro-inflammatory cytokines found in atherosclerotic plaque was assessed at the molecular level. VSC preparations from C57BL/6 and $ApoE^{-/-}$ mice were induced to undergo chondrogenesis by exposure to transforming growth factor (TGF)-β3 and bone morphogenetic protein (BMP)-2 in a 3D format in the presence or absence of interleukin (IL)-6, IL-1β or tumor necrosis factor (TNF)-α. The effect of the cytokines on temporal patterns of expression of characteristic matrix components during endochondral ossification was analyzed to identify the factors that potentially modulate vascular calcification *in vivo*.

## Materials and Methods

### MSC and VSC Isolation, Culture and Characterization

All animal procedures were conducted in a fully accredited housing facility under a license granted by the Department of Health, Ireland and were approved by the Animal Care and Research Ethics Committee at the National University of Ireland Galway, Ireland. $ApoE^{-/-}$ MSCs were isolated as described previously with minor modifications [7]. Successful cultures

of bone marrow-derived MSCs from C57BL/6 mice were established using modifications of a previously described procedure [16]. The isolation of VSC from ApoE$^{-/-}$ and C57BL/6 aortas was adopted from the protocol described by da Silva Meirelles and Nardi [7]. Briefly, dissected aortas with extraneous tissue removed were digested with collagenase twice with the second cell fraction used to establish cultures in RPMI-1640 medium with supplements. Subsequent to P2, cultures were transferred to MSC medium. Detailed information on isolation and growth analysis as well as isolation of fibroblasts is provided in supplementary data.

**Surface Marker Analysis**

Cells at P6 were analyzed for surface marker expression using the FACSCanto (Becton Dickinson). Antibodies used for flow cytometry are listed in the supplementary methods. Data were analyzed by FlowJo software (Tree Star Inc.) using appropriate controls with isotype-matched IgG and unstained samples. Immunohistochemical staining for 3G5, a cell surface ganglioside typically found on vascular pericytes [17] was performed. 3G5 positive cells were purified from an ApoE$^{-/-}$ VSC preparation using fluorescence activated cell sorting as detailed in supplementary data.

**Multilineage Potential**

MSCs and VSCs were evaluated for osteogenic, chondrogenic and adipogenic differentiation. Osteogenic differentiation was assessed by determination of calcium phosphate deposition using von Kossa staining after 14 days in osteogenic differentiation medium [18] and calcium quantitation was assessed using Calcium Liquicolour Kit (StanBio, Boerne, TX, USA). For adipogenic differentiation analysis, Oil Red O staining was performed on cells cultured for 20 days in adipogenic induction medium. For chondrogenesis, cell pellets were digested with papain and glycosaminoglycan (GAG) determined using the dimethylmethylene blue assay (DMMB). Histological sections (5μm) of formalin-fixed pellets were stained for the presence of GAG using toluidine blue. Immunocytochemistry for type II and X Collagen was performed for

establishment of the chondrogenic phenotype. All procedures are described in detail in the supplementary information.

**Animal Study and Histology**

To study effects of the atherosclerotic environment and intrinsic capacity of the cells to differentiate *in vivo*, chondrogenically-primed constructs were implanted subcutaneously into C57BL/6 control and atherosclerotic ApoE$^{-/-}$ mice that had been fed a Western diet. The seeding of scaffolds and chondrogenic priming of constructs are detailed in supplementary methods. For direct comparison, chondrogenically-primed and control-unprimed constructs, loaded with either MSC or VSC from each mouse strain were implanted in C57BL/6 and ApoE$^{-/-}$ mice (n=8 constructs). All mice were euthanized 8 weeks post-implantation and retrieved constructs were processed histologically. Four serial sections were cut at 4-8 levels at least 100μm apart and stained with haematoxylin/eosin. To quantify bone formation in the implanted constructs, a robust histological grading/scoring system was developed to assess the extent of three distinct features of differentiation: calcified cartilage, bone and bone marrow formation. Sections from each animal and each treatment were randomized to eliminate bias and scored for each feature by three independent, blinded researchers. The grading system involved assessment of bone formation by allotting an overall bone score on the scale of 0-4 for the three parameters, with 0 indicating no tissue was detected and 4 indicating 100% fill of the construct. The overall bone score was defined as the sum of individual calcified cartilage, bone and bone marrow scores. This bone score was used to define the percentage of overall bone formation with score of 4 set as 100%. The scoring system is detailed in supplementary Table 1. Sections were also stained with Safranin O and Collagen Type X to visualize hypertrophic cartilage.

**Effect of Pro-inflammatory Cytokines on Chondrogenic Differentiation of VSCs**

The effect of pro-inflammatory cytokines on chondrogenic differentiation of VSCs from ApoE$^{-/-}$ and C57BL/6 mice was assessed. Pellet cultures were established in chondrogenic medium with

or without treatment with 200ng/mL IL-6 [19], 1ng/mL IL-1β [20] or 10ng/mL TNF-α [20] (Peprotech) for 48h, and 7, 14 and 21 days. Gene expression of the chondrogenic markers Sox9, Fibromodulin, Type II collagen, Aggrecan (ACAN), Runx2, Alkaline phosphatase (ALP) and Type X collagen was assessed. See supplementary data for detailed procedures.

**Statistical Analysis**

Data are expressed as the mean ± standard deviation (SD). All experiments were performed in triplicate, unless otherwise noted. Statistical significance was tested using Student's *t* test or ANOVA followed by Tukey's test. P value of $\leq 0.05$ was set as the cut off for statistical significance.

**Results**

**Characterization of the Pericyte Nature of MSCs and VSCs**

Bone marrow-derived MSCs and aorta-derived VSCs, isolated from C57BL6 and $ApoE^{-/-}$ mice showed a similar fibroblastic morphology (Figure 1A). The proliferation profile of the cell populations was assessed from passage P6/7 to P14. Doubling times calculated for all three independent pooled preparations from $ApoE^{-/-}$ MSCs and VSCs as well as C57BL/6 VSCs show a strong similarity. C57BL/6 MSCs did display slower growth characteristics (Supplementary Table 1). Assessment of mouse MSC-, pericyte-, hematopoietic- and endothelial-associated cell surface markers was performed to define the surface signature of the isolated populations. Representative histograms for MSC and pericyte-associated markers are shown in Figure 1B and supplementary Table 1 summarizes results obtained using three individual cell preparations. All VSCs and MSCs were negative for endothelial and hematopoietic cell markers but were positive for the previously described MSC markers Sca-1 [21, 22] and CD44 [21], although the latter was detected at a lower intensity (Figure 1B). CD90.2 was detected in a low percentage of MSCs but present in VSCs. To further assess the pericyte nature of the cells, expression of the

pericyte markers, CD146 and 3G5, was investigated (Figure 1B and 1C). VSCs showed some positivity for CD146 while MSCs were negative. Likewise, the presence of 3G5 was associated with VSCs, although detected at lower levels by both flow cytometry (Figure 1B) and immunofluorescent staining of cultured cells (Figure 1C). Conversely, CD140b was detected at high levels in both MSC preparations (>90%) but at lower levels in C57BL/6 VSCs (57.2%) compared to Apo$^{-/-}$ VSCs (70.2%) (Supplementary Table 2 and Supplementary Figure 1). All MSC and VSC preparations were negative for Tie-2 (Figure 1B).

**The *In Vivo* Atherosclerotic Environment Increases the Ability of VSCs and MSCs to Generate a Calcified Matrix *In Vitro***

The ability of MSCs and VSCs, isolated from ApoE$^{-/-}$ and C57BL/6 mice, to generate a calcified matrix through direct intramembranous ossification or endochondral ossification, via a cartilage intermediate, was investigated. When treated with osteogenic supplements to induce direct ossification, all preparations showed the presence of a mineralized matrix by Von Kossa staining. Staining was more pronounced in VSCs and MSCs from ApoE$^{-/-}$ mice compared to cells from C57BL/6 mice (Figure 2Ai and Supplementary Figure 2). Quantification of calcium elaborated in the matrix indicated that levels were significantly higher in cells from ApoE$^{-/-}$ mice compared to the respective cells from C57BL/6 mice (Figure 2Aii).

VSCs and MSCs from both mouse strains were induced to undergo chondrogenic differentiation by exposure to BMP-2 and TGF-β3 for 21 days in 3D culture, as a model for the first stages of endochondral ossification. In general, ApoE$^{-/-}$ MSC and VSC pellets tended to be larger in size compared to respective C57BL/6 pellets. The matrix generated was analyzed for glycosaminoglycan (GAG) using toluidine blue staining and quantitation by dimethylmethylene blue (DMMB). All treated preparations were positive for GAG with metachromatic staining in pellets generated from ApoE$^{-/-}$ cells comparatively more intense (Figure 2Bi). At higher

magnification, hypertrophic cells were observed to be embedded in the proteoglycan rich matrix.

Sequential sections from the center of pellets were immunostained for type II and type X collagen to confirm chondrogenesis and hypertrophic differentiation, respectively. Type II collagen staining was detected primarily in the periphery of MSC pellets but more generally expressed in VSC chondrogenic cultures. Localization of type X collagen correlated with type II collagen. Although all pellet cultures showed abundant accumulation of type II and X collagen at 21 days, staining appeared greater in the $ApoE^{-/-}$ MSC and VSC pellets (Figure 2Bi). The GAG/DNA ratio in $ApoE^{-/-}$ MSC and VSC pellets was also significantly higher when compared to respective C57BL/6 pellets (Figure 2Bii), indicating either increased synthesis and/or low turnover per cell. Overall, VSCs and MSCs from $ApoE^{-/-}$ mice had significantly higher *in vitro* chondrogenic potential compared to control mice. Fibroblasts, isolated from adult $ApoE^{-/-}$ and C57BL/6 mouse skin and lung tissue, did not undergo osteogenesis and formed loose pellets that were not possible to evaluate for chondrogenic differentiation. Supplementary Figure 3 shows negative staining for calcium post osteogenic differentiation of $ApoE^{-/-}$ and C57BL/6 lung fibroblasts. $ApoE^{-/-}$ MSCs, used as a positive control, were positive for both osteo- and chondrogenesis (results not shown).

As 3G5 positive cells ($3G5^+$) have been shown to differentiate to bone and cartilage [23], $3G5^+$ and $3G5^-$ VSCs were sorted to 100% purity and compared to the parent $ApoE^{-/-}$ VSC population with respect to chondrogenic differentiation. The parent and sorted cell populations were expanded for 2 passages to obtain sufficient cell numbers and exposed to chondrogenic medium for 21 days. $3G5^+$ cells formed a cohesive pellet with positive metachromatic staining and hypertrophic cells detected (white arrow). Parent cells also showed positive GAG staining. Conversely, $3G5^-$ cells formed a loose pellet compared to the $3G5^+$ pellets with weak GAG staining. With respect to GAG/DNA levels, $3G5^+$ cells produced over 1.5 fold more GAG than

the parent and $3G5^-$ cells (12.3 ± 0.4, 8.1 ± 0.1 and 7.2 ±0.5 μg/μg GAG/DNA, respectively) (Supplementary Figure 4).

Following adipogenic differentiation, accumulation of lipid droplets was visualized in C57BL/6 MSCs using Oil Red O staining whereas $ApoE^{-/-}$ MSCs and VSCs were negative for adipogenic differentiation (data not shown).

**Assessment of the Intrinsic Calcification Capacity of Progenitor Cells *In Vivo* and the Effect of the Atherosclerotic Environment**

To assess calcification of progenitor cells *in vivo*, passage (P)8 MSCs and VSCs from both mouse strains were loaded on collagen-glycosaminoglycan scaffolds [15] and pre-differentiated in chondrogenic medium for 32 days prior to subcutaneous implantation. Cell-scaffold constructs maintained in control culture medium for 32 days served as negative controls. A crossover experimental plan was used where cells from each strain were implanted in C57BL/6 and $ApoE^{-/-}$ mice (Supplementary Figure 5).

Control and chondrogenically-primed constructs were stained with toluidine blue to assess the quality of seeding. Cells were found distributed throughout the constructs; however, cell density was higher at the edges. In all seeded, chondrogenically-primed constructs, weak matrix staining for GAG was evident whereas the controls showed no GAG deposition (Supplementary Figure 6). Not all implanted constructs were retrievable with control cultures recovered at a lower frequency. The gross appearance of primed constructs is presented in Supplementary Figure 7 with vascularization and a bony appearance evident. Representative sections were stained with Safranin O and collagen type X to confirm the appearance of hypertrophic cartilage (Supplementary Figures 8 and 9).

**$ApoE^{-/-}$ MSCs and VSCs Form Bone in C57BL/6 Mice**

When chondrogenically-primed constructs from atherosclerotic mice were transplanted into subcutaneous pouches of control mice, all MSC- or VSC-seeded constructs underwent

mineralization and formed bone (Table 1A and B, Figure 3A). In the case of the primed ApoE$^{-/-}$ MSC constructs retrieved from C57BL/6 mice, 5 of 5 retrieved constructs had evident bone formation. The overall bone formation was 77.5% with more than 20% of bone marrow formation suggesting areas of maturity. However, the presence of 25% calcified cartilage indicated areas of less mature bone. Chondrogenically-primed ApoE$^{-/-}$ VSC constructs retrieved from C57BL/6 mice formed bone or immature bone in 5 of 5 retrieved samples. In 3 of 5 constructs, bone marrow was seen (Figure 3A). Of the 58.4% overall bone formation score, 25% was immature bone with calcified cartilage while 17.75% bone marrow was present. In summary, bone marrow-derived MSCs, with known bone forming capacity, demonstrated a greater capacity for bone formation post-chondrogenic priming than VSCs from the same atherosclerotic background.

**The Atherosclerotic Environment Complements the Intrinsic Capacity of ApoE$^{-/-}$ MSCs and VSCs to Form Bone**

To investigate how the intrinsic capacity of MSCs and VSCs from atherosclerotic mice is affected by the atherosclerotic environment, the fate of the ApoE$^{-/-}$ constructs in ApoE$^{-/-}$ mice was assessed. Quantification of overall bone formation is detailed in Table 1 (A and B). All 5 constructs of primed ApoE$^{-/-}$ MSCs retrieved from atherosclerotic mice formed bone and bone marrow. With prominent dense bone appearance (30%), calcified matrix (23.5%) and areas with bone marrow (15%), the overall bone formation was rated at 68.5%. A large number of hypertrophic cells were observed surrounded by cartilage-like matrix containing bone like tissue components and invading blood vessels (Figure 3B and Table 1A). Of note, un-primed control ApoE$^{-/-}$ MSC constructs retrieved from atherosclerotic mice also formed some bone with 18% of overall bone formation and 10.25% cartilage observed in 2 of 4 retrieved constructs. Total bone marrow observed was 4.75% and seen in 2 of 4 retrieved constructs (Table 1A).

The examination of 6 of 6 primed ApoE$^{-/-}$ VSCs in the ApoE$^{-/-}$ environment showed the presence of osteoid tissue with a number of hypertrophic cells embedded in a cartilaginous matrix; notably, all constructs showed invading blood vessels (Figure 3B and Table 1B). The bone appearance was dense with 83.25% overall bone formation and the presence of a calcified matrix was prominent with 24% coverage. In all treated ApoE$^{-/-}$ constructs retrieved from ApoE$^{-/-}$ mice, substantial formation of bone marrow was observed (34%), revealing the maturity of the developed bone. Similar to ApoE$^{-/-}$ MSCs explanted from atherosclerotic mice, un-primed ApoE$^{-/-}$ VSCs formed some bone (18%) in atherosclerotic mice (Table 1B). Detection of significant levels of calcified cartilage in both conditions suggested endochondral ossification as the primary pathway for bone formation. That both unprimed atherosclerotic MSCs and VSCs formed bone when exposed to the diseased environment and primed atherosclerotic VSCs generated about 25% more bone highlights the effect of the atherosclerotic environment on the calcifying potential of vessel progenitor cells.

**The Atherosclerotic Environment Positively Impacts Bone Formation Capacity of C57BL/6 Cells**

For ApoE$^{-/-}$ MSC (4 of 4) and C57BL/6 MSC (4 of 4) control constructs retrieved from control mice, there was no bone, cartilage or bone marrow formation (Table 1A). Two of 5 C57BL/6 MSC control constructs retrieved from atherosclerotic mice had overall bone formation at 5%. Of this, 3% was calcified cartilage with no bone marrow observed (Figure 4 and Table 1A). This analysis of non-atherosclerotic constructs retrieved from the atherosclerotic environment indicated a modest role of the atherosclerotic environment alone. In the case of primed C57BL/6 MSCs retrieved from atherosclerotic mice, overall new bone formation was 18.75%. 2 of 5 constructs formed some bone while 3 of 5 constructs showed an average of 9.25% calcified cartilage (Figure 4 and Table 1A). However, un-primed C57BL/6 VSCs were unable to form

bone in either mouse strain (Figure 4, Table 1B) suggesting that vessel-resident progenitor cells do not have intrinsic capacity to form bone.

**Effect of IL-6, IL-1β or TNF-α on Pattern of Expression During Chondrogenesis**

*In vivo* data highlighted the relevance of the source of progenitor cells to their calcification/bone formation potential, with the inflammatory milieu of the atherosclerotic ApoE$^{-/-}$ mouse altering the intrinsic calcification capacity of ApoE$^{-/-}$ cells. Short term implantation in this inflammatory environment also resulted in increased bone capacity of C57BL/6 MSCs, although not VSCs. To determine putative factors involved in establishing the atherosclerotic progenitor cell phenotype we investigated the effect of IL-6, IL-1β and TNF-α on chondrogenesis of VSCs. Pellet cultures were established from ApoE$^{-/-}$ and C57Bl/6 VSCs and treated with chondrogenic induction medium supplemented with 200ng/mL IL-6, 1ng/mL IL-1β or 10ng/mL TNF-α treatment. Chondrogenically-cultured pellets without cytokine treatment acted as controls.

In terms of morphology, ApoE$^{-/-}$ and C57BL/6 VSC pellets treated with chondrogenic induction medium alone for 21 days and stained with toluidine blue had the characteristic blue-pink appearance indicating the presence of GAG (Figure 5A). GAG/DNA levels were equivalent between the two populations (Figure 5B and C). C57BL/6 VSC pellets treated with inflammatory cytokines were smaller in appearance with minimal GAG detected histologically and quantitatively (Figure 5A and B). GAG/DNA levels were significantly reduced by exposure to IL-6, IL-1β and TNF-α compared to controls. Treatment with 200ng/mL IL-6 caused a reduction in GAG production; treatment with 1ng/mL IL-1β or 10ng/mL TNF-α further impacted chondrogenic differentiation of C57BL/6 VSCs with significantly reduced GAG levels compared to the IL-6-treated pellets (Figure 5B).

After 21 days chondrogenic pellet culture in the presence of pro-inflammatory cytokines, ApoE$^{-/-}$ VSCs had a distinct chondrogenic appearance/morphology. Notably, the IL-6 treated pellets were larger than control cultures treated with chondrogenic medium alone (Figure 5A).

This increased size correlated with significantly higher GAG/DNA levels (Figure 5C), whereas exposure to 1ng/mL IL-1β or 10ng/mL TNF-α had no effect compared to controls. Glycosaminoglycan deposition after exposure to IL-6 was significantly higher compared to all other treatments (Figure 5C).

The effect of 200ng/mL IL-6 on expression of the chondrogenic-associated molecules, Sox-9 and fibromodulin, as well as collagen type II and aggrecan at 21 days was found to be significantly higher in ApoE$^{-/-}$ VSCs compared to C57BL/6 VSCs treated with 200ng/mL IL-6 (Figure 6A-D). Similarly, IL-6 addition led to a significant increase in gene expression of *Runx2* and *ALP*, markers of chondrocyte hypertrophy, in ApoE$^{-/-}$ VSCs compared to C57BL/6 VSCs at 21 days (Figure 6E, F). Significance was also seen at day 2 for *Runx2* and day 7 for *ALP*. However, treatment with IL-6 led to decreased collagen type X expression, also associated with hypertrophy and generation of a transient cartilage template in endochondral ossification, in both ApoE$^{-/-}$ and C57BL6 VSCs compared to control cultures (Figure 6G). The treatment with either IL-1β or TNF-α showed a trend towards decreased expression of all chondrogenic genes tested compared to control cultures (data not shown).

**Discussion**

In recent years, dogmas of not only repair and regeneration but disease progression are changing rapidly with identification of various stem/progenitor cells in the vessel wall. One target cell population is the MSC, described as a pericyte or pericyte-like cell and proposed to have a perivascular origin [6, 24, 25]. Although current knowledge of vessel-derived progenitor cells is in its infancy, much attention has focused on their therapeutic application for conditions such as myocardial infarction, ischemic heart disease and limb ischemia. The contribution of altered stem or progenitor cell function to disease development is also of interest with reports of dysfunction in bone marrow-derived endothelial progenitor cells, fibrocytes, pericytes, MSCs or smooth muscle progenitor cells contributing to atherosclerosis and vascular calcification [23,

26-29]. There is also increasing evidence that the vessel wall, including the vascular intima or adventitia, is the seat for resident stem progenitor cells [30] which can be induced to calcify [31]. Evidence also suggests the presence of progenitor cells in tunica media which can transdifferentiate into smooth muscle cells and contribute to vascular remodeling in atherosclerosis [32].

The aim of this study was to identify, isolate and characterize a population of resident stem/ progenitor cells from the aortic wall of young atherosclerotic mice and to assess their role in the pathogenesis of atherosclerosis. VSCs were shown to be capable of differentiating into bone and cartilage and were fundamentally altered by the atherosclerotic environment. These cells were compared to bone marrow-derived MSCs to elucidate their potential contribution to formation of ectopic bone or cartilage in atherosclerotic plaque. Resident progenitors were associated with a more pericyte-like phenotype compared to matched MSCs, circulating progenitor cells that may contribute to vascular calcification in plaque [33]. Indeed, both MSCs and VSCs from atherosclerotic mice were shown to display significantly higher capacity to form a cartilaginous template and directly ossify *in vitro* compared to control cells from non-atherosclerotic, wild type mice. However, $ApoE^{-/-}$VSCs had a greater chondrogenic capacity than the same cells isolated from C57BL/6 mice. *In vivo*, formation of prominent and mature bone-like structures in chondrogenically-primed $ApoE^{-/-}$ VSC and MSC constructs, even in a non-atherosclerotic environment, suggested an intrinsic proclivity of these cells to form ectopic bone, which in the case of VSCs was boosted even further in the atherosclerotic environment. This notion was further supported by the observation that the MSCs from control mice, whether primed or not, were substantially less prone to form bone even in the atherosclerotic environment. In contrast to MSCs isolated from bone marrow which have a known functional role in bone formation, VSCs isolated from the aorta of C57BL/6 mice did not have the capacity to form bone or calcify *in vivo* indicating that these vessel-derived progenitors do not have bone forming capacity in the

non-diseased environment. However, ApoE$^{-/-}$ VSCs that were primed to undergo chondrogenesis prior to subcutaneous implantation in control mice formed bone. Metaplasia and calcification occurs in the aortic tunica. It is now known that this abnormality is not just a physical accumulation of calcium phosphate, but involves mechanisms similar to bone formation with a number of bone-related proteins expressed within the vessel wall [11]. The presence of calcified cartilage and bone in the majority of constructs where differentiation of implanted cells occurred, and particularly in unprimed constructs, suggests that endochondral ossification was the primary pathway involved. Differentiation and calcification of constructs in the atherosclerotic environment may be regulated by exposure to various factors like TNF-α or IL-6 which may also play role in formation of the plaque and atherogenesis [34]. To date, a number of researchers have reported the presence of stem cells in blood vessels including the aorta [7]. Their regenerative role in injury is well known, however our work was based on the premise that they can also be implicated in pathological processes under certain conditions. The mechanism whereby this occurs is not fully understood. The potential of vessel wall stem cells to form bone, cartilage, muscle or fat has been reported previously [35]. More specifically, the cells which are isolated form aortic tunicae have a greater tendency to differentiate to the osteogenic lineage [35, 36] upon exposure to inflammatory cytokines.

In both environments, ApoE$^{-/-}$ cells were prone to calcify and develop bone structures; nevertheless VSCs were more sensitive to environmental factors. The ApoE$^{-/-}$ environment seemed to contribute to mature bone formation in the ApoE$^{-/-}$ primed constructs but to a lesser degree in control non-primed constructs. Interestingly, the ApoE$^{-/-}$ environment also triggered bone formation in C57BL/6 control constructs, even without priming, albeit to a much lesser degree, again supporting the hypothesis that the atherosclerotic environment plays a role in differentiation and ectopic bone formation. The importance of the atherosclerotic environment in bone formation becomes even more obvious by the observation that control constructs retrieved from the control non-atherosclerotic environment did not form bone. Nevertheless, the

finding that there was some bone formation in primed C57BL/6 constructs retrieved from control mice, was similar to findings in Balb/C mice [37] and rats [38]. Previously, it has been shown that cells subjected to differentiation assays will usually down regulate bone and chondrogenic transcription factors under pro-inflammatory conditions [20]. In this study, we found that the pro-inflammatory environment of the atherosclerotic mice did not inhibit the formation of bone in subcutaneous implants but exaggerated the effect leading to more advanced calcification, particularly in the case of VSCs. In the atherosclerotic environment, a number pro-inflammatory cytokines such as TNF-α, IL-6, IL-1β are increased [39] and inflammatory cytokines are strongly related to ectopic bone formation [40].

What triggers the inflammatory reaction in atherosclerosis is not completely understood. However, numerous factors such as oxidized LDL, free oxygen radicals and to some extent, MMPs, heat shock proteins and advanced glycation end products have been implicated. Data presented here help to understand the regulatory mechanisms that link pericytes/VSCs and ectopic calcification. Although the role of factors other than inflammatory cytokines in promoting bone formation or calcification *in vivo* cannot be ignored, the significant inhibitory effect of IL-6, IL-1β and TNFα on proteoglycan production in C57BL/6 control VSC chondrogenesis in vitro compared to no effect of IL-1β and TNFα, and significantly increased chondrogenic and hypertrophic gene expression as well as overall GAG levels in response to IL-6 in $ApoE^{-/-}$ VSCs does indicate that these pro-inflammatory cytokines, upregulated in the atherosclerotic environment, can modulate VSC chondrogenesis. Overall, there was over 2-fold more GAG/DNA produced by $ApoE^{-/-}$ VSCs compared to control C57BL6 VSCs. Similarly, Lacey et al. have demonstrated that mouse MSCs, differentiated in the presence of pro-inflammatory cytokines, had decreased chondrogenic and osteogenic gene expression and both IL-1β and TNF-α have been shown to significantly inhibit chondrogenesis of human MSCs [20, 41, 42]. Furthermore, these factors potently inhibit expression of Sox 9, the master

chondrogenic transcription factor through the NF-κB pathway [43]. As for control C57BL/6 VSCs, IL-6 has also been shown to inhibit chondrogenesis of healthy human MSCs [44, 45]. In this study, we have shown for the first time that the ApoE$^{-/-}$ VSCs have the ability to respond to IL-6 treatment and induce accumulation of proteoglycans. The difference between ApoE$^{-/-}$ VSCs and C57BL/6 VSCs was also apparent visually with IL-6-treated ApoE$^{-/-}$ VSC pellets appearing larger than control cultures in contrast to the TNF-α and IL-1β treated pellets. IL-6 has also been shown to induce calcification of SMCs. In a co-culture model, increased expression of TNF-α and IL-6 in macrophages induced SMC calcification in a paracrine manner [43]. The atheroprotective and anti-calcific effects of osteoprotegerin (OPG) have also been associated with receptor activator of NF-κB ligand (RANKL) modulation of IL-6 production [45]. In this study vascular smooth muscle cells from ApoE$^{-/-}$OPG$^{-/-}$ mice showed increased chondrogenic differentiation and elevated IL-6 levels in response to RANKL treatment and decreased calcification after ablation of RANKL signalling. Moreover, increased expression of IL-6 has been associated with human calcific aortic valve disease and phosphate-induced mineralization of mouse valve interstitial cells was dependent on IL-6 [46]. The NF-κB pathway was also implicated on IL-6-associated mineralization in this study. With respect to the contribution of the diseased environment to altered responses to cytokines, a recent study described an amplification autocrine loop involving IL-6 and basic calcium phosphate crystal in promoting calcification associated with experimental osteoarthritis: the increased production of IL-6 was mediated partially through STAT 3 and PI3 kinase [47].

The molecular analysis in this study was based on markers signifying three progressive phases of chondrogenesis. Thus, the significant upregulation of key genes in chondrogenesis in ApoE$^{-/-}$ VSCs in the presence of IL-6 at different stages of chondrogenic differentiation reveals that this cytokine plays a central pathological role in the atherosclerotic microenvironment. Although VSCs do not normally calcify *in vivo* they possess a differentiation potential which is

responsive to cytokines and makes them capable of formation of ectopic bone in aortae. The differentiation of ApoE$^{-/-}$ VSCs in the presence of IL-6 to chondrocytes characterized in this study and the temporal changes observed in gene expression largely paralleled the pattern of extensive calcification *in vivo* occurring in atherosclerosis. Sequential gene expression patterns which closely regulate cell-cell and cell-matrix interactions leading to alterations at morphological and metabolic levels during development of cartilage [48] are not only mirrored during deposition of calcified matrix in the atherogenic processes but also to some extent during commitment of VSCs to the endochondral pathway.

Taken together, it is clear from this study that endochondral ossification and calcification in atherosclerosis is a complex interplay of a number of factors, each contributing differently to the process. It can be concluded that a major contributing factor is the intrinsic capacity of MSCs and VSCs derived from atherosclerotic mice to calcify. Nonetheless, this study also demonstrated that the environment in which cells are pre-differentiated and the actual host environment drive the implanted constructs to form bone or premature bone, bone marrow, calcified cartilage and promote infiltration of blood vessels. This study also revealed that in the presence of pro-inflammatory cytokines, IL-6 in particular, released by surrounding or localized inflammatory cells, ApoE$^{-/-}$ VSCs may become more permissive to this microenvironment and commit to the chondrogenic differentiation pathway leading to endochondral ossification.

**Acknowledgments**

The authors thank Dr. Xizhe Chen for his assistance and technical contribution and Dr. Shirley Hanley for assistance with flow cytometry.

**Sources of Funding**

This work was supported by the Irish Research Council for Science, Engineering and Technology and Science Foundation Ireland under Grant No. 09/SRC/B1794.

## Disclosures

None.

## References


1. Gomez-Gaviro MV, Lovell-Badge R, Fernandez-Aviles F et al. The vascular stem cell niche. **J Cardiovasc Transl Res**. 2012;5:618-630.
2. Torsney E, Xu Q. Resident vascular progenitor cells. **J Mol Cell Cardiol**. 2011;50:304-311.
3. Klein D, Weisshardt P, Kleff V et al. Vascular wall-resident CD44+ multipotent stem cells give rise to pericytes and smooth muscle cells and contribute to new vessel maturation. **PLoS One**. 2011;6:e20540.
4. Zengin E, Chalajour F, Gehling UM et al. Vascular wall resident progenitor cells: a source for postnatal vasculogenesis. **Development**. 2006;133:1543-1551.
5. Tonlorenzi R, Dellavalle A, Schnapp E et al. Isolation and characterization of mesoangioblasts from mouse, dog, and human tissues. **Curr Protoc Stem Cell Biol**. 2007;Chapter 2:Unit 2B 1.
6. Crisan M, Yap S, Casteilla L et al. A perivascular origin for mesenchymal stem cells in multiple human organs. **Cell Stem Cell**. 2008;3:301-313.
7. da Silva Meirelles L, Chagastelles PC, Nardi NB. Mesenchymal stem cells reside in virtually all post-natal organs and tissues. **J Cell Sci**. 2006;119:2204-2213.
8. Alexopoulos N, Raggi P. Calcification in atherosclerosis. **Nature reviews Cardiology**. 2009;6:681-688.
9. Rajamannan NM, Bonow RO, Rahimtoola SH. Calcific aortic stenosis: an update. **Nature clinical practice Cardiovascular medicine**. 2007;4:254-262.
10. Johnson RC, Leopold JA, Loscalzo J. Vascular calcification: pathobiological mechanisms and clinical implications. **Circulation research**. 2006;99:1044-1059.
11. Fukagawa M, Kazama JJ. The making of a bone in blood vessels: from the soft shell to the hard bone. **Kidney Int**. 2007;72:533-534.
12. Li R, Mittelstein D, Lee J et al. A dynamic model of calcific nodule destabilization in response to monocyte- and oxidized lipid-induced matrix metalloproteinases. **Am J Physiol Cell Physiol**. 2012;302:C658-665.
13. Farrington-Rock C, Crofts NJ, Doherty MJ et al. Chondrogenic and adipogenic potential of microvascular pericytes. **Circulation**. 2004;110:2226-2232.
14. Greenow K, Pearce NJ, Ramji DP. The key role of apolipoprotein E in atherosclerosis. **J Mol Med**. 2005;83:329-342.
15. Farrell E, van der Jagt OP, Koevoet W et al. Chondrogenic priming of human bone marrow stromal cells: a better route to bone repair? **Tissue engineering Part C, Methods**. 2009;15:285-295.
16. Sudres M, Norol F, Trenado A et al. Bone marrow mesenchymal stem cells suppress lymphocyte proliferation in vitro but fail to prevent graft-versus-host disease in mice. **J Immunol**. 2006;176:7761-7767.
17. Nayak RC, Berman AB, George KL et al. A monoclonal antibody (3G5)-defined ganglioside antigen is expressed on the cell surface of microvascular pericytes. **The Journal of experimental medicine**. 1988;167:1003-1015.
18. Neuhuber B, Gallo G, Howard L et al. Reevaluation of in vitro differentiation protocols for bone marrow stromal cells: disruption of actin cytoskeleton induces rapid

morphological changes and mimics neuronal phenotype. **J Neurosci Res**. 2004;77:192-204.
19. Parhami F, Basseri B, Hwang J et al. High-density lipoprotein regulates calcification of vascular cells. **Circulation research**. 2002;91:570-576.
20. Lacey DC, Simmons PJ, Graves SE et al. Proinflammatory cytokines inhibit osteogenic differentiation from stem cells: implications for bone repair during inflammation. **Osteoarthritis Cartilage**. 2009;17:735-742.
21. Halfon S, Abramov N, Grinblat B et al. Markers distinguishing mesenchymal stem cells from fibroblasts are downregulated with passaging. **Stem Cells Dev**. 2011;20:53-66.
22. Houlihan DD, Mabuchi Y, Morikawa S et al. Isolation of mouse mesenchymal stem cells on the basis of expression of Sca-1 and PDGFR-alpha. **Nat Protoc**. 2012;7:2103-2111.
23. Canfield AE, Doherty MJ, Wood AC et al. Role of pericytes in vascular calcification: a review. **Z Kardiol**. 2000;89 Suppl 2:20-27.
24. Crisan M, Chen CW, Corselli M et al. Perivascular multipotent progenitor cells in human organs. **Annals of the New York Academy of Sciences**. 2009;1176:118-123.
25. Howson KM, Aplin AC, Gelati M et al. The postnatal rat aorta contains pericyte progenitor cells that form spheroidal colonies in suspension culture. **Am J Physiol Cell Physiol**. 2005;289:C1396-1407.
26. Vasuri F, Fittipaldi S, Pasquinelli G. Arterial calcification: Finger-pointing at resident and circulating stem cells. **World journal of stem cells**. 2014;6:540-551.
27. Iwata H, Manabe I, Nagai R. Lineage of bone marrow-derived cells in atherosclerosis. **Circulation research**. 2013;112:1634-1647.
28. Ruan C, Shen Y, Chen R et al. Endothelial progenitor cells and atherosclerosis. **Front Biosci (Landmark Ed)**. 2013;18:1194-1201.
29. Cabbage S, Ieronimakis N, Preusch M et al. Chlamydia pneumoniae infection of lungs and macrophages indirectly stimulates the phenotypic conversion of smooth muscle cells and mesenchymal stem cells: potential roles in vascular calcification and fibrosis. **Pathogens and disease**. 2014.
30. Ergun S, Tilki D, Klein D. Vascular wall as a reservoir for different types of stem and progenitor cells. **Antioxid Redox Signal**. 2011;15:981-995.
31. Yang S, Eto H, Kato H et al. Comparative characterization of stromal vascular cells derived from three types of vascular wall and adipose tissue. **Tissue Eng Part A**. 2013;19:2724-2734.
32. Tang Z, Wang A, Yuan F et al. Differentiation of multipotent vascular stem cells contributes to vascular diseases. **Nature communications**. 2012;3:875.
33. Wang W, Li C, Pang L et al. Mesenchymal stem cells recruited by active TGFbeta contribute to osteogenic vascular calcification. **Stem Cells Dev**. 2014;23:1392-1404.
34. Yan J, Stringer SE, Hamilton A et al. Decorin GAG synthesis and TGF-beta signaling mediate Ox-LDL-induced mineralization of human vascular smooth muscle cells. **Arteriosclerosis, thrombosis, and vascular biology**. 2011;31:608-615.
35. Demer LL, Tintut Y. Vascular calcification: pathobiology of a multifaceted disease. **Circulation**. 2008;117:2938-2948.
36. Abedin M, Tintut Y, Demer LL. Mesenchymal stem cells and the artery wall. **Circ Res**. 2004;95:671-676.
37. Farrell E, Both SK, Odorfer KI et al. In-vivo generation of bone via endochondral ossification by in-vitro chondrogenic priming of adult human and rat mesenchymal stem cells. **BMC Musculoskelet Disord**. 2011;12:31.
38. Yang W, Yang F, Wang Y et al. In vivo bone generation via the endochondral pathway on three-dimensional electrospun fibers. **Acta biomaterialia**. 2013;9:4505-4512.

39. Hansson GK. Inflammation, atherosclerosis, and coronary artery disease. **N Engl J Med**. 2005;352:1685-1695.
40. Sage AP, Tintut Y, Demer LL. Regulatory mechanisms in vascular calcification. **Nature reviews Cardiology**. 2010;7:528-536.
41. Heldens GT, Blaney Davidson EN, Vitters EL et al. Catabolic factors and osteoarthritis-conditioned medium inhibit chondrogenesis of human mesenchymal stem cells. **Tissue Eng Part A**. 2012;18:45-54.
42. Murakami S, Lefebvre V, de Crombrugghe B. Potent inhibition of the master chondrogenic factor Sox9 gene by interleukin-1 and tumor necrosis factor-alpha. **The Journal of biological chemistry**. 2000;275:3687-3692.
43. Deuell KA, Callegari A, Giachelli CM et al. RANKL enhances macrophage paracrine pro-calcific activity in high phosphate-treated smooth muscle cells: dependence on IL-6 and TNF-alpha. **J Vasc Res**. 2012;49:510-521.
44. Pricola KL, Kuhn NZ, Haleem-Smith H et al. Interleukin-6 maintains bone marrow-derived mesenchymal stem cell stemness by an ERK1/2-dependent mechanism. **J Cell Biochem**. 2009;108:577-588.
45. Callegari A, Coons ML, Ricks JL et al. Increased calcification in osteoprotegerin-deficient smooth muscle cells: Dependence on receptor activator of NF-kappaB ligand and interleukin 6. **J Vasc Res**. 2014;51:118-131.
46. El Husseini D, Boulanger MC, Mahmut A et al. P2Y2 receptor represses IL-6 expression by valve interstitial cells through Akt: implication for calcific aortic valve disease. **J Mol Cell Cardiol**. 2014;72:146-156.
47. Nasi S, So A, Combes C et al. Interleukin-6 and chondrocyte mineralisation act in tandem to promote experimental osteoarthritis. **Ann Rheum Dis**. 2015.
48. Kronenberg HM. Developmental regulation of the growth plate. **Nature**. 2003;423:332-336.

## Figure Legends

**Figure 1. Characterization of isolated stem cell populations. A,** Morphology of MSCs and VSCs isolated from ApoE$^{-/-}$ and C57BL/6 background mice. Representative images at P7 showed a characteristic spindle-like, fibroblastic appearance. Scale bar, 200μm. **B,** Immunophenotypic profile of C57BL/6 and ApoE$^{-/-}$ MSCs and VSCs at P6. Surface marker expression (red line) for Sca-1, CD44, CD90.2, CD146, 3G5 and Tie-2 compared to respective isotype controls (blue line). **C,** Immunocytochemistry showing distribution of 3G5 positive MSCs and VSCs from both mouse strains; scale bar, 32μm.

**Figure 2. Osteogenic and Chondrogenic differentiation of stem cell populations. A,** MSCs and VSCs isolated from C57BL/6 and ApoE$^{-/-}$ mice underwent osteogenesis as demonstrated macroscopically by positive Von Kossa staining (i) and quantitatively by assessment of calcium deposition (ii). Cells cultured in control medium were negative; scale bar, 500μm. **B (**i) Chondrogenesis was assessed for proteoglycan deposition by toluidine blue staining after 21 days in pellet culture (top two panels with magnified insets taken from the regions indicated, scale bars 500 and 200μm, respectively) and for the presence of collagen type II and X (scale bars, 200μm). (ii) GAG/DNA ratios for isolated pellets. (n= 3 cell preparations; *, ** $P \leq 0.05$).

**Figure 3. The atherosclerotic environment and bone forming capacity of isolated progenitors. A,** All chondrogenically primed ApoE$^{-/-}$ MSC and VSC constructs retrieved from C57BL/6 mice showed mineralization and bone formation (black stars). **B,** Primed ApoE$^{-/-}$ MSC and VSC constructs retrieved from ApoE$^{-/-}$ mice showed more mature bone formation with well-developed bone marrow (yellow arrowheads) and blood vessels (red arrowheads) detected. Boxes indicated areas magnified. Left panels, 100μm magnification; right panels, 50μm).

**Figure 4. Effect of atherosclerotic environment on non-atherosclerotic C57BL/6 cells** Control, unprimed C57BL/6 MSC constructs implanted into ApoE$^{-/-}$ mice showed calcified cartilage and some bone formation (black stars). Comparatively, primed C57BL/6 MSC constructs showed more bone formation with marrow like spaces. Control and chondrogenically-primed C57BL/6 VSC constructs implanted in to ApoE$^{-/-}$ mice showed no bone formation while remnants of scaffolds (red stars) were seen. Scale bars, 50μm.

**Figure 5. Effect of pro-inflammatory cytokines on chondrogenesis of ApoE$^{-/-}$ and C57BL/6 VSCs. A,** The effect of treatment with IL-6 (200ng/ml), for 21 days on proteoglycan deposition during chondrogenic differentiation of C57BL/6 and ApoE$^{-/-}$ VSCs is visualized by toluidine blue staining (Scale bars, 200μm) and **B,** quantified by determination of GAG/ DNA ratio (n= 3 cell preparations; **P* < 0.01, ***P* < 0.02, $^{¥}$*P* < 0.05).

**Figure 6. Effect of IL-6 on expression of representative chondrogenic genes during differentiation of ApoE$^{-/-}$ and C57BL/6 VSCs.** Isolated cells were differentiated in chondrogenic conditions in the presence or absence of IL-6 (200ng/ml) and cultured in pellet format for 21 days. Gene expression normalized to GAPDH of **A,** Sox9, **B,** fibromodulin, **C,** type II collagen, **D,** ACAN, **E,** Runx2, **F,** ALP and **G,** type X collagen at time 0, and 48 hour, 7 day, 14 day and 21 day pellets (n=5) in chondrogenic medium. Data represents the relative expression seen after exposure to IL-6 compared to control cultures exposed to chondrogenic medium without IL-6 (n=3 cell preparations, 2 technical replicates; **P* < 0.03, ***P* < 0.02).

**Table 1. Histological analysis of (A) MSC and (B) VSC constructs retrieved from ApoE$^{-/-}$ and C57BL/6 mice scored for bone, calcified cartilage and bone marrow formation.** Constructs were stained with H&E staining for light microscopic evaluation and grading by three blinded reviewers. Numbers represent constructs showing the presence of the particular feature out of the total number of retrieved constructs. Numbers in brackets indicate the average score of the three assessments for the presence of bone, calcified cartilage and marrow and overall bone score the sum of these values. Overall bone formation was calculated from the summed mean scores with 4 representing 100% coverage.

**Supplementary Figure Legends**

**Supplementary Figure 1. Cell surface phenotype of VSCs and MSCs.** The cells were phenotyped using flow cytometry for the negative MSCs markers, CD34, CD45, CD105, CD31 and the perivascular cell marker CD140b. Representative staining of MSCs and VSCs from C57BL/6 and ApoE$^{-/-}$ mice are displayed as histograms (red line- surface antigens and blue line- negative controls ).

**Supplementary Figure 2. Mineralization potential of isolated preparations.** Representative Von Kossa staining of C57BL/6 and ApoE$^{-/-}$ MSCs and VSCs 14 days post-osteogenic induction. Cells cultured in control medium were negative; Scale bar, 500μm.

**Supplementary Figure 3. Osteogenic potential of lung fibroblasts from C57BL/6 and ApoE$^{-/-}$ mice.** Lung fibroblasts from either strain did not undergo osteogenic differentiation as visualized by lack of Von Kossa staining at day 14 post induction of osteogenesis. Scale bar, 200μm.

**Supplementary Figure 4. Isolated VSCs were sorted by flow cytometry for expression of 3G5 and cell populations were characterized for chondrogenic differentiation**. i) Viable cells were selected by the forward versus side scatter profile (a), with dead cells excluded by gating using 7-AAD (b), doublets by the single cell gate (c) and debris by the scatter gate (d). The isotype control and 3G5 sort gates are shown in e) and f), respectively where p5 is negative and p6 positive. Purity of each population was shown to be g) 100% negative and h) 100% positive. Sorted positive and negative 3G5 cells were subjected to chondrogenic assays. Parent VSCs (i) showed chondrogenic morphology whereas the negative fraction (j) did not form a defined pellet and the 3G5$^{+}$ sorted cells (k) formed a hypertrophic pellet. Scale bar, 200μm. ii)

$3G5^+$ cell fraction also had higher a GAG/DNA ratio compared to parent $ApoE^{-/-}$ VSCs and $3G5^-$ sorted cells (n= 3 technical replicates).

**Supplementary Figure 5. Experimental design**. Control, unprimed or chondrogenically-primed $ApoE^{-/-}$ and C57BL/6 MSCs and VSCs constructs were implanted subcutaneously in the back of C57BL/6 and $ApoE^{-/-}$ mice.

**Supplementary Figure 6. Assessment of collagen-glycosaminoglycan scaffolds prior to *in vivo* implantation.** Toluidine Blue staining showing homogenous cell distribution in both control and chondrogenically-primed constructs after 32 days in culture (Low and high magnification, 200μm and 50μm; red arrowheads, scaffold).

**Supplementary Figure 7. Gross appearance of retrieved samples.** After 8 weeks implantation, the level of bone formation, bone marrow as well as blood vessels and fat appearance in the retrieved constructs was analysed. Grossly, (i), (ii) chondrogenically primed $ApoE^{-/-}$ MSC constructs retrieved from C57BL/6 mice appeared vascularized. (iii), (iv) chondrogenically primed $ApoE^{-/-}$ MSC constructs retrieved from $ApoE^{-/-}$ mice had the appearance of hard bone-like structures. (v), (vi) chondrogenically primed $ApoE^{-/-}$ VSC constructs retrieved from C57BL/6 mice. (vii), (viii) chondrogenically primed $ApoE^{-/-}$ VSC constructs retrieved from $ApoE^{-/-}$ mice. These retrieved constructs seemed to have the appearance of hard bone-like structures and exhibited vascularization. Scale, 1 division - 1mm.

**Supplementary Figure 8. Histologic and immunohistochemical characterization of retrieved constructs from C57BL/6 and $ApoE^{-/-}$ from primed and unprimed MSCs and VSCs**. A, Representative Safranin-O red staining of primed $ApoE^{-/-}$ MSC and VSC constructs

retrieved from ApoE$^{-/-}$ mice showing mature bone formation with well-developed bone marrow. Scale bars, 200μm. B, Histological examination of un-primed and primed C57BL/6 constructs retrieved from ApoE$^{-/-}$ mice. H&E and Safranin-O red staining were used to analyze matrix synthesis and GAG deposition, respectively.

**Supplementary Figure 9. Bone and matrix formation in primed ApoE$^{-/-}$ MSC and VSC constructs retrieved from C57BL/6 and ApoE$^{-/-}$ mice by type X collagen staining.** Positive immunohistochemical localization of type X collagen, a marker of chondrocyte hypertrophy, is evident in the chondral portion of the constructs (Scale bars, 200μm).

**Supplementary Figure 10. Electropherograms (Agilent Bioanalyzer) from control and treated samples showing total RNA integrity**. All scans show high quality and intact total RNA with RIN (RNA Integrity Number) equal to 10.

**Supplementary Table 1. Growth profile of cell populations.** Doubling time (days) was calculated from three independent isolations for all cell preparations using data from the passages (P) indicated.

**Supplementary Table 2. Surface characteristics of isolated cells by flow cytometry.** Values are presented as the mean ±SD of 3 preparations and represent percentage of positive cells.

**Supplementary Table 3. Histological grading scale for subcutaneous retrieved samples.** The grading score took in to account the appearance of bone, cartilage, bone marrow, fat, fibrous matrix and blood vessel formation as well as surrounding host tissue.

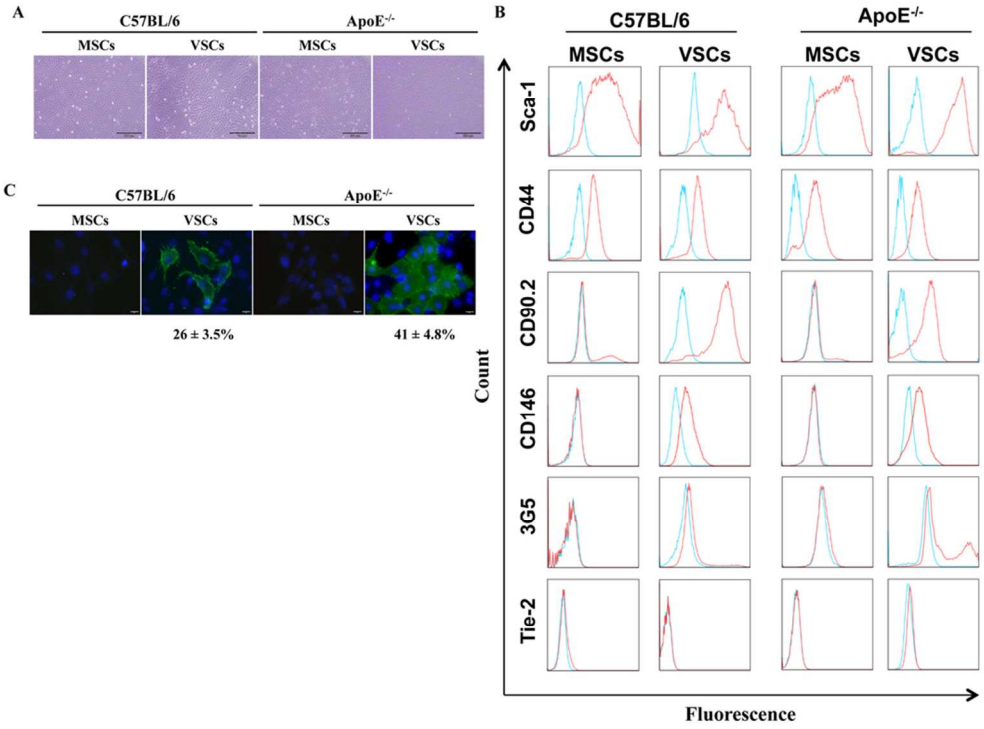


Figure 1. Characterization of isolated stem cell populations. A, Morphology of MSCs and VSCs isolated from ApoE-/- and C57BL/6 background mice. Representative images at P7 showed a characteristic spindle-like, fibroblastic appearance. Scale bar, 200μm. B, Immunophenotypic profile of C57BL/6 and ApoE-/- MSCs and VSCs at P6. Surface marker expression (red line) for Sca-1, CD44, CD90.2, CD146, 3G5 and Tie-2 compared to respective isotype controls (blue line). C, Immunocytochemistry showing distribution of 3G5 positive MSCs and VSCs from both mouse strains; scale bar, 32μm.
91x67mm (300 x 300 DPI)

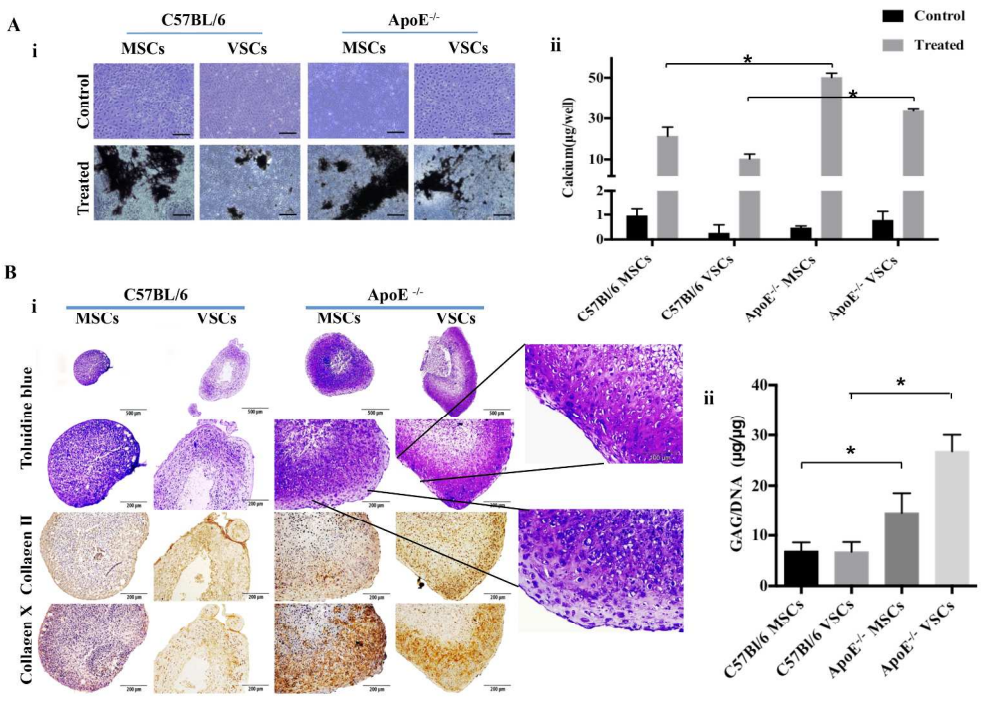


Figure 2. Osteogenic and Chondrogenic differentiation of stem cell populations. A, MSCs and VSCs isolated from C57BL/6 and ApoE-/- mice underwent osteogenesis as demonstrated macroscopically by positive Von Kossa staining (i) and quantitatively by assessment of calcium deposition (ii). Cells cultured in control medium were negative; scale bar, 500µm. B (i) Chondrogenesis was assessed for proteoglycan deposition by toluidine blue staining after 21 days in pellet culture (top two panels with magnified insets taken from the regions indicated, scale bars 500 and 200µm, respectively) and for the presence of collagen type II and X (scale bars, 200µm). (ii) GAG/DNA ratios for isolated pellets. (n= 3 cell preparations; *, ** P≤0.05).
251x181mm (300 x 300 DPI)

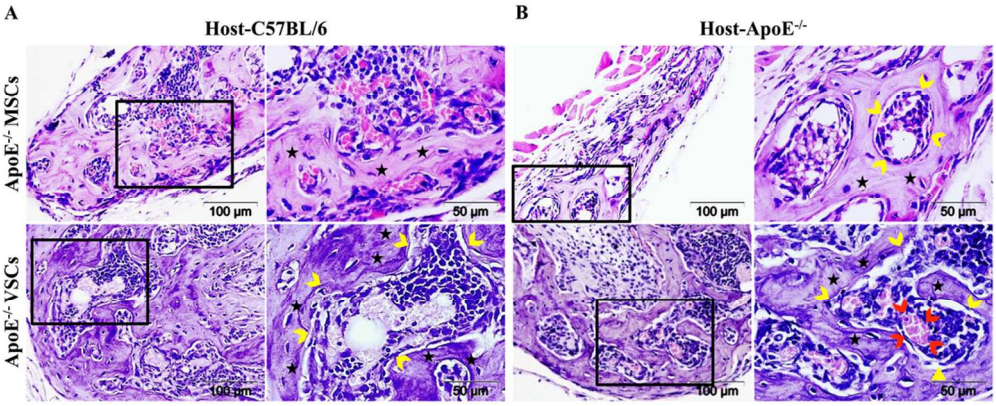


Figure 3. The atherosclerotic environment and bone forming capacity of isolated progenitors. A, All chondrogenically primed ApoE-/- MSC and VSC constructs retrieved from C57BL/6 mice showed mineralization and bone formation (black stars). B, Primed ApoE-/- MSC and VSC constructs retrieved from ApoE-/- mice showed more mature bone formation with well-developed bone marrow (yellow arrowheads) and blood vessels (red arrowheads) detected. Boxes indicated areas magnified. Left panels, 100µm magnification; right panels, 50µm).
102x42mm (300 x 300 DPI)

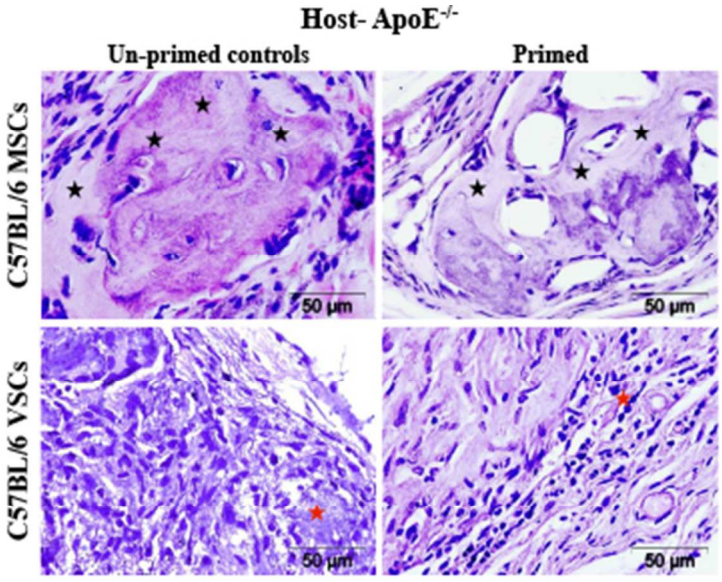


Figure 4. Effect of atherosclerotic environment on non-atherosclerotic C57BL/6 cells\r\nControl, unprimed C57BL/6 MSC constructs implanted into ApoE-/- mice showed calcified cartilage and some bone formation (black stars). Comparatively, primed C57BL/6 MSC constructs showed more bone formation with marrow like spaces. Control and chondrogenically-primed C57BL/6 VSC constructs implanted in to ApoE-/- mice showed no bone formation while remnants of scaffolds (red stars) were seen. Scale bars, 50µm.
31x26mm (300 x 300 DPI)

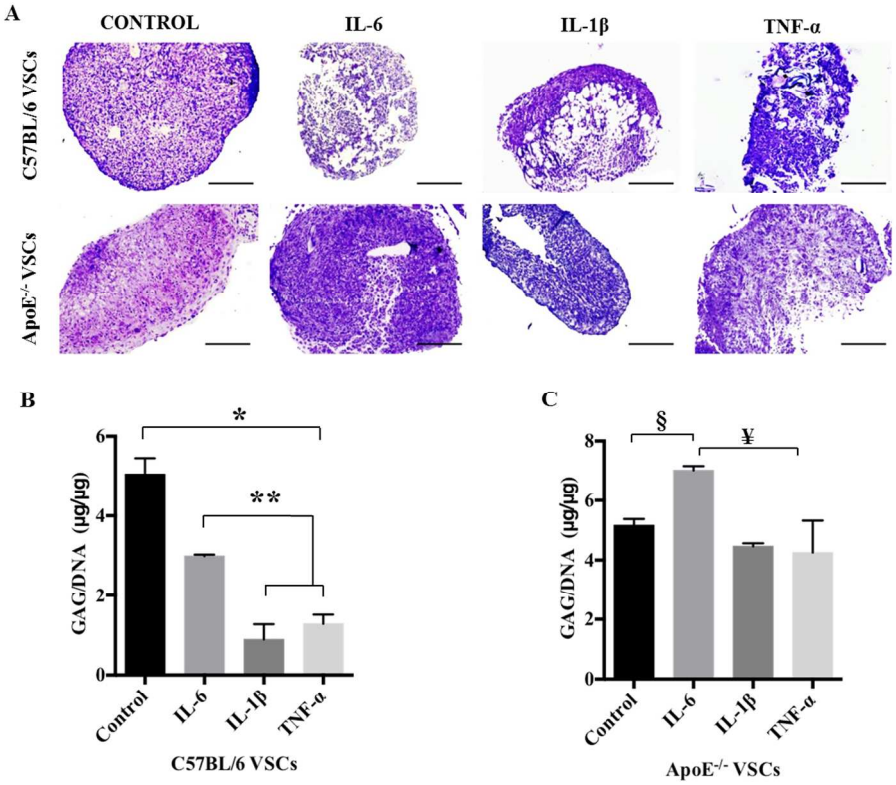


Figure 5. Effect of pro-inflammatory cytokines on chondrogenesis of ApoE-/- and C57BL/6 VSCs. A, The effect of treatment with IL-6 (200ng/ml), for 21 days on proteoglycan deposition during chondrogenic differentiation of C57BL/6 and ApoE-/- VSCs is visualized by toluidine blue staining (Scale bars, 200μm) and B, quantified by determination of GAG/ DNA ratio (n= 3 cell preparations; *P < 0.01, **P < 0.02, ¥P < 0.05).
212x169mm (300 x 300 DPI)

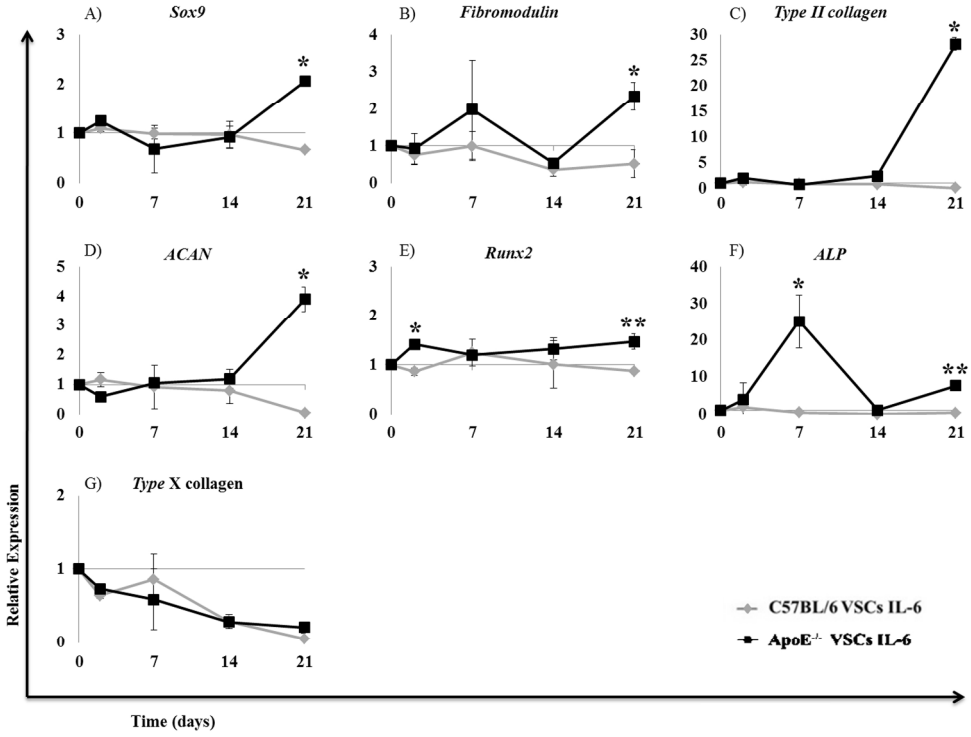


Figure 6. Effect of IL-6 on expression of representative chondrogenic genes during differentiation of ApoE-/- and C57BL/6 VSCs. Isolated cells were differentiated in chondrogenic conditions in the presence or absence of IL-6 (200ng/ml) and cultured in pellet format for 21 days. Gene expression normalized to GAPDH of A, Sox9, B, fibromodulin, C, type II collagen, D, ACAN, E, Runx2, F, ALP and G, type X collagen at time 0, and 48 hour, 7 day, 14 day and 21 day pellets (n=5) in chondrogenic medium. Data represents the relative expression seen after exposure to IL-6 compared to control cultures exposed to chondrogenic medium without IL-6 (n=3 cell preparations, 2 technical replicates; *P < 0.03, **P < 0.02).
254x190mm (300 x 300 DPI)

**Table 1. Histological analysis of (A) MSC and (B) VSC constructs retrieved from ApoE$^{-/-}$ and C57BL/6 mice scored for bone, calcified cartilage and bone marrow formation.** Constructs were stained with H&E staining for light microscopic evaluation and grading by three blinded reviewers. Numbers represent constructs showing the presence of the particular feature out of the total number of retrieved constructs. Numbers in brackets indicate the average score of the three assessments for the presence of bone, calcified cartilage and marrow and overall bone score the sum of these values. Overall bone formation was calculated from the summed mean scores with 4 representing 100% coverage.

**A**

| Host | | | Implanted cells: ApoE $^{-/-}$ MSCs control | ApoE $^{-/-}$ MSCs primed | C57BL/6 MSCs control | C57BL/6 MSCs primed |
|---|---|---|---|---|---|---|
| ApoE $^{-/-}$ | | Calcified Cartilage | 2/4 (0.41) | 5/5 (0.94) | 1/5 (0.12) | 3/5 (0.37) |
| | | Bone | 2/4 (0.12) | 5/5 (1.2) | 2/5 (0.08) | 2/5 (0.24) |
| | | Bone Marrow | 2/4 (0.19) | 5/5 (0.6) | 0/5 (0) | 1/5 (0.14) |
| | | Overall Bone Score | 0.72 | 2.74 | 0.2 | 0.75 |
| | | Percentage of overall bone formation | 18% | 68.5% | 5% | 18.75% |
| C57BL6 | | Calcified Cartilage | 0/4 (0) | 5/5 (1.27) | 0/4 (0) | 1/4 (0.23) |
| | | Bone | 0/4 (0) | 5/5 (0.99) | 0/4 (0) | 1/4 (0.15) |
| | | Bone Marrow | 0/4 (0) | 5/5 (0.84) | 0/4 (0) | 0/4 (0) |
| | | Overall Bone Score | 0 | 3.1 | 0 | 0.38 |
| | | Percentage of overall bone formation | 0% | 77.5% | 0% | 9.5% |

**B**

| Host | | | Implanted cells: ApoE $^{-/-}$ VSCs control | ApoE $^{-/-}$ VSCs primed | C57BL/6 VSCs control | C57BL/6 VSCs primed |
|---|---|---|---|---|---|---|
| ApoE $^{-/-}$ | | Calcified Cartilage | 3/4 (0.32) | 6/6 (0.96) | 0/4 (0) | 0/4 (0) |
| | | Bone | 3/4 (0.27) | 6/6 (1.01) | 0/4 (0) | 0/4 (0) |
| | | Bone Marrow | 1/4 (0.13) | 6/6 (1.36) | 0/4 (0) | 0/4 (0) |
| | | Overall Bone Score | 0.72 | 3.33 | 0 | 0 |
| | | Percentage of overall bone formation | 18% | 83.25% | 0% | 0% |
| C57BL/6 | | Calcified Cartilage | 1/6 (0.023) | 5/5 (1) | 0/4 (0) | 0/6 (0) |
| | | Bone | 0/6 (0) | 5/5 (0.63) | 0/4 (0) | 0/6 (0) |
| | | Bone Marrow | 0/6 (0) | 3/5 (0.71) | 0/4 (0) | 0/6 (0) |
| | | Overall Bone Score | 0.023 | 2.34 | 0 | 0 |
| | | Percentage of overall bone formation | 0.583% | 58.4% | 0% | 0% |

**NOTE:** Constructs were stained with H&E staining for light microscopic evaluation and grading by three blinded reviewers. Numbers represent constructs showing the presence of the particular feature out of the total number of retrieved constructs. Numbers in brackets indicate the average score of the three assessments for the presence of bone, calcified cartilage and marrow and overall bone score the sum of these values. Overall bone formation was calculated from the summed mean scores with 4 representing 100% coverage.

**SUPPLEMENTARY MATERIAL**

**Supplementary Methods**

**Cell isolation**

*Isolation of ApoE$^{-/-}$ MSCs from bone marrow.* Mouse MSCs were isolated as described previously with minor modifications [1]. Briefly, bone marrow was obtained from 8 to 12-week old ApoE$^{-/-}$ mice. Marrow plugs were transferred to Dulbecco's modified Eagle's medium (DMEM) supplemented with 10% fetal bovine albumin (FBS), 10mmol/L HEPES, 100U/mL penicillin and 100μg/mL streptomycin (1% P/S) dispersed by repeated pipetting. The bone marrow mononuclear cell (BMMNC) fraction was washed twice by centrifugation (400g, 10 minutes) at room temperature (RT) before plating at $2\times10^6$ BMMNC/cm$^2$ and cultured in a humidified 5% $CO_2$ incubator at 37°C for 72 hours. Medium was changed to remove non-adherent cells and cultures fed every 3-4 days. Colonies were established over 22 to 25 days and were passaged to avoid overgrowth. On subculture cells were re-plated at $5\times10^3$ cells/cm$^2$ with subsequent passages established with $2.8\times10^3$ cells/cm$^2$. Cultures were passaged at 70-80% confluence and culture medium was changed every 3–4 days.

*Isolation of C57BL/6 MSCs from bone marrow.* The protocol for isolation of mMSCs from ApoE$^{-/-}$ mouse marrow, as described above, was unsuccessful for C57BL/6 mice. Successful cultures were ultimately established using modifications of the procedure described by Sudres et al.[2] Marrow plugs were obtained from femur and tibia of 8 to 12 week old C57BL/6 mice, transferred to α-MEM supplemented with 1% P/S and 10% FBS and dispersed by repeated pipetting. BMMNC were filtered through a 70mm mesh and washed twice by centrifugation at 400g for 6 minutes in α-MEM supplemented with 1% P/S prior to re-suspension in complete medium. Cells were plated at $5\times10^6$ cells/cm$^2$ and incubated in a humidified atmosphere at 33°C and 5% $CO_2$. After 48 hours, non-adherent cells were removed by

washing with phosphate-buffered saline (PBS) and fresh medium was added. The temperature of the incubation was raised by one degree every 3-4 days until it reached 37ºC. Medium was changed weekly until cultures were near confluence when cells were washed with PBS and detached using trypsin/EDTA for 2-3 minutes at 37°C. Cells were expanded by plating at $4\times10^3$ cells/cm$^2$ and passaged at 70-80% confluence in subsequent passages at $2.8\times10^3$ cells/cm$^2$.

*Isolation of VSCs from the aortas of ApoE$^{-/-}$ and C57BL/6 mice.* Isolation of VSC from ApoE$^{-/-}$ was adopted from the protocol described by da Silva Meirelles and Nardi [1]. Briefly, the ascending aorta was dissected, cleaned and transferred to DMEM/HEPES without FBS containing Antibiotic/Antimycotic (100U/mL penicillin, 100ug/mL streptomycin and 0.25µg/mL amphotericin B) in a Petri dish and cut into small pieces. The dissected pieces (around 0.2-0.8cm$^3$) were washed with DMEM/HEPES, cut into smaller fragments, and digested with 10mL of collagenase type I (0.5mg/mL in DMEM/HEPES) for 30 minutes at 37°C. The aorta was digested for around 30 minutes and subjected to vigorous agitation, yielding a first cell fraction. The remnant of the vessel was then washed in 20mL DMEM/HEPES, and transferred to a new tube for a second collagenase digestion yielding a second cell fraction. For establishment of the cultures (passage 0 to 2), second cell fraction was grown in RPMI supplemented with 10% FBS, 10% Horse Serum (HS), 1% L-glutamine and 1% P/S. Subsequently, DMEM supplemented with 0.01M HEPES, 10% FBS and 1% P/S was used.

*Isolation of fibroblasts from m*ouse *lung and skin.* Fibroblasts were isolated as previously described by Seluanov et al. 2010 [3].

*Cell growth analysis.* Population doublings and doubling time were determined based on the number of cells plated and harvested versus the duration of culture time in days. Cumulative population doublings were calculated with respect to cell numbers obtained from passage 6 or 7 to 14. To maintain the same

conditions across different cell preparations, medium changes were done at a set interval of 3 to 4 days and cells were harvested at 80% of confluence.

**Flow Cytometric Surface Marker Characterisation of MSCs and VSCs**

For cell surface marker analysis all cell preparations at passage 6 and 80% confluence were trypsinised and resuspended in PBS containing 2% FBS and 1mM EDTA (FACS) buffer. The following monoclonal antibodies were used for flow cytometric analysis: Anti-CD31 (clone MEC 13.3, PE), anti-CD34 (clone RAM34, PE), anti-CD45 (clone 30-F11, PE), anti-CD117 (clone ACK45, PE), anti-CD44 (clone IM7, PE), anti-Sca-1 (clone E13-161.7, PE), anti-CD90.2 (clone 30-H12, PE), anti-CD105 (clone MJ7/18, PE, eBioscience), anti-Tie-2 (clone TEK4, PE, BioLegend) and anti-CD146 (clone ME-9F1, PE, BioLegend) and isotype controls. Histograms of the cell number versus fluorescence intensity were recorded with $5\times10^4$ cells per sample and analyzed using FlowJo (Tree Star Inc.) software. Expression of each marker was presented as percentage of the total population calculated from number of cell expressing the marker verses control unstained cells.

**Fluorescence activated cell sorting of the 3G5-expressing cell subpopulation from ApoE$^{-/-}$ VSCs**

ApoE$^{-/-}$ VSC were sorted using the FACSAariaII (BD). Passage 8 cultures were trypsinized at 80% confluency and resuspended in PBS with 10% FBS and 5% NGS for 30min on ice. The 3G5 hybridoma supernatant was added with 10% FBS for incubation overnight. The cells were washed and the secondary antibody (goat FITC Anti- mouse IgM) at a 1:100 dilution in 10% FBS added for 45min. The cells were washed twice in FACS buffer, resuspended in the required volume of FACS buffer and filtered via a 70μm cell strainer. The dead cells were excluded by 7-amino-actinomycin D (7-AAD). The 3G5$^+$ and 3G5$^-$ cell fractions were gated or analyzed based on fluorescence minus one (FMO) and isotype controls for 3G5 expression. The single cell gate was set to remove any doublets and the scatter gate to ensure the

any debris or dead cells were excluded. Sorted cells were re-analysed to ensure high purity. Immunohistochemistry for 3G5 antigen was performed to ensure that all cells were 3G5 positive prior to further analysis.

**Immunofluorescence**

To prepare the 3G5 primary antibody, CRL-1814 (ATTC) hybridoma was used. Briefly, hybridoma cells were grown in DMEM supplemented with 10% FBS in an incubator for 2 weeks to get optimum proliferation of the cells. Diminution of FBS levels in the medium was achieved by a 1% reduction every 5-7 days until 0.5% FBS was obtained. The final culture was left for 5 days. The culture was then poured into sterile 50mL tubes and the supernatant harvested by centrifuging for 20 minutes at 1,500g at RT. Supernatant was collected to fresh tubes and stored at -80ºC. The presence of IgM antibody was confirmed by mouse IgM specific IsoQuick strips and western blotting.

VSCs and MSCs were plated at $3\times10^3$ cells per chamber in a 4-well chamber slide and cultured for 3 days. Live cells were blocked with 10% normal goat serum (NGS) and 1% bovine serum albumin (BSA) in PBS for 1 hour. Cells were then incubated overnight with non-diluted primary 3G5 antibody at 4°C. Following the incubation, cells were washed twice with 1% BSA in PBS for 5 minutes and incubated with FITC-conjugated goat anti mouse secondary antibody (Sigma; SAB4700348) for 1 hour at 4°C. After washing twice with 1% BSA for 5 minutes, the cells were fixed with 4% paraformaldehyde (PFA) for 15 minutes and washed twice with PBS for 5 minutes. Cells were incubated with 0.8mM Hoechst solution for 30 sec to 1 minute. Two washings with PBS for 5 minutes were performed and the slides were mounted using Vectashield mounting medium H-1000 (Vector Laboratories). The proportion of cells positive for 3G5 was quantified using image analysis software (Image-Pro® Plus 7.0, Media Cybernetics). For controls, nonspecific monoclonal mouse IgM antibody was substituted for the primary antibody. Images were captured using an Olympus BX51 Upright Fluorescent Microscope with an

Improvision Optigrid System. For the flow cytometry analysis, VSCs from ApoE$^{-/-}$ and C57BL/6 were resuspended in FACS buffer following overnight incubation with primary 3G5 antibody. The cells were incubated with FITC-conjugated anti-mouse IgM for 45 minutes and analyzed using the FACSCanto.

**Multilineage Potential**

MSCs and VSCs were expanded up to 6 passages, and then evaluated for differentiation capacity as follows.

*Osteogenic differentiation.* To induce osteogenic differentiation, MSCs and VSCs were seeded into 6-well plates at a density of $1.3\times10^4$ cells/well and cultured for 24 hours. Cells were then placed in osteoblastic differentiation medium for 14 days (Iscove's medium supplemented with 100nM dexamethasone, 10mM beta-glycerophosphate, and 50μM ascorbic acid, 10% FBS and Antibiotic/Antimycotic) (Sigma). Cells were maintained in induction medium for 14 days with media changes every 2 days. Cells cultured in complete MSC/VSC growth media were used as controls. Quantification of calcium deposition was performed by a colorimetric calcium assay (Calcium CPC Liquicolour, Stanbio Inc.).

Briefly, standards ranging from 0.05μg/mL to 1.5μg/mL were prepared in 0.5M HCl. After washing the samples twice with DPBS, 0.5M HCl was added to each well. The contents were scraped into eppendorf tubes, shaken overnight at 4ºC and centrifuged at 1,000g for 5 minutes. 200μl of Stanbio Calcium (CPC) Liquicolor working solution (1:1 working dye to binding reagent) was added to standards and samples in a 96-well plate and incubated at RT for 15 minutes in the dark. Absorbance readings were performed in duplicate at 550nm on a Wallac Victor3™ 1420 Multilabel Counter spectrophotometer and standard curve was used to quantify the levels.

Von Kossa staining was carried out for calcium deposition in the osteogenic cultures. Briefly, cultures were washed twice with PBS and fixed with 4% PFA for 20 minutes prior to exposure to 3% silver nitrate solution in darkness at RT for 10 minutes. Cells were rinsed three times with $dH_2O$ and exposed to bright light for 15 minutes. Cells were rinsed again and photographed on an Olympus IX71 inverted microscope camera utilizing Cell IP imaging software (Olympus). A silver black color confirmed the presence of calcium deposits.

*Chondrogenic differentiation.* To induce chondrogenic differentiation, the harvested MSCs and VSCs were washed sequentially in PBS and chondrogenic medium without growth factors and resuspended in chondrogenic medium at $5x10^4$ cells/pellet, prior to centrifugation for 5 minutes at 100g in sterile polypropylene round-bottom 96-well plates. Complete chondrogenic medium (CCM) consisted of high glucose DMEM supplemented with 100nM dexamethasone, 1mM sodium pyruvate, 50µg/mL 2-phosphate ascorbic acid, 40µg/mL L-proline, 1% Insulin-Transferrin-Selenium (ITS) supplement , 100ng/mL bone morphogenetic protein 2 (BMP-2) (R&D Systems), 10ng/mL transforming growth factor beta 3 (TGF-β3) (R&D Systems) and antibiotic/antimycotic. Medium was changed every 2 days for 3 weeks. After washing in PBS, pellets were fixed in 10% neutral buffered formalin for 1 hour and paraffin-embedded. Deparafinized sections (5µm) were stained with 0.03% toluidine blue for 5 minutes at 60ºC to visualize sulfated proteoglycans (GAG). GAG concentration was quantified on chondrogenic pellets after 21 days using dimethylmethylene blue (DMMB). Pellets were digested in 0.0025mg/mL papain solution at 60°C overnight. Digests were used for measurement of GAG and DNA. Picogreen® assay was used for DNA and DMMB dye assay was used for GAG content. Total amount of GAG was normalized against the total amount of DNA.

**Type II and X collagen immunohistochemistry**

Deparaffinized sections were washed with PBS and digested for 40 minutes at RT with 0.1% pepsin in 0.2M HCl and/or 25mg/mL hyaluronidase in PBS for collagen type II with only 0.1% of pepsin in 0.5M acetic acid for collagen type X. After several washings with PBS, sections were treated with 1% $H_2O_2$ in methanol for 30 minutes to block endogenous peroxidase activity. Nonspecific binding was blocked using 10% normal goat serum (NGS) and 5% BSA for 1 hour in a humidity chamber followed by overnight incubation with collagen II or X antibody (Gentaur; LSL LB -1297 at 1:1000; LSL LB-0092 at 1:1000) at 4°C. The sections were treated with biotin-labeled anti-rabbit goat IgG (Dako E0432 at 1:200) for 35 minutes at RT followed by peroxidase labeled streptavidin (Dako) for 30 minutes at 1:200 and RT. A diaminobenzidine (DAB) tablet was dissolved in 15mL PBS, filtered and activated prior to use by 12 µl of $H_2O_2$. After development with DAB the sections were counterstained in hematoxylin for 30 sec. Slides were mounted with DPX mountant and imaged using an upright brightfield microscope (Olympus BX51 Upright Fluorescent Microscope with Improvision Optigrid System). Negative controls were subjected to the same protocol with omission of primary antibody.

***In vivo* assessment of bone formation**

*Scaffold seeding.* Collagen glycosaminoglycan (collagen GAG) scaffolds were seeded with P8 MSCs or VSCs from C57BL/6 and ApoE$^{-/-}$ mice as described previously [4]. Briefly, 100µl of a $5\times10^6$ cells/mL solution was gently pipetted onto one surface of the collagen GAG scaffolds and incubated for 30 minutes. Scaffolds were then inverted onto agar-coated wells (2mL of 2% autoclaved agarose gel per well; LE analytical grade, Promega) and an additional 100µl of cell suspension placed onto the samples. After a further 30 minutes, 3mL of their respective cell culture medium was added. Scaffolds were cultured for 32 days in chondrogenic medium.

*Subcutaneous implantation of chondrogenically-primed constructs.* All animal procedures were conducted in a fully accredited housing facility under a license granted by the Department of Health,

Ireland and were approved by the Animal Care and Research Ethics Committee at the National University of Ireland Galway, Ireland. Pre-differentiated constructs were implanted subcutaneously into 8 weeks old C57BL/6 control mice and atherosclerotic ApoE$^{-/-}$ mice that had been fed a Western diet since birth. For assessment of bone formation, chondrogenically-primed and control constructs, loaded with MSC or VSC from each mouse strain, were implanted in C57BL/6 and ApoE$^{-/-}$ mice (n=8 constructs). Empty scaffold controls were also implanted. Constructs were randomly assigned to implantation position. All mice were euthanized 8 weeks post-implantation and retrieved constructs washed twice in PBS and fixed in 10% neutral buffered formalin for 1 hour. The explanted samples were subsequently decalcified in 10% EDTA at pH 8. Samples were embedded in paraffin before cutting at a thickness of 5µm (Leica RM2235) for analysis. Four serial sections (5µm) were cut at 4-8 levels at least 100µm apart.

*RNA extraction and Real-Time PCR.* The effect of pro-inflammatory cytokines on the chondrogenic differentiation of VSCs from ApoE$^{-/-}$ and C57BL/6 mice was assessed. Pellet cultures of these cells were established in chondrogenic medium with or without treatment with IL-6 (200ng/mL) [5], IL-1β (1ng/mL) [6] or TNF-α (10ng/mL) [6] (Peprotech) for 48 hours, 7 days, 14 days and 21 days. Total RNA was isolated using RNeasy kit (Qiagen) according to manufacturer's instructions after 0, 2, 7, 14 and 21 days pellet culture with n=5 pellets per time point. cDNA stocks for each sample were synthetized using the Im-prom- IITM reverse transcription system (Promega) analyzed for gene expression via Fast SYBR® Green Master Mix (Applied Biosystems). Data with primers sets specific for Sox9 (Forward: 5'tatcttcaaggcgctgcaa'3; Reverse: 5'tcggttttgggagtggtg'3), Fibromodulin (Forward: 5'cagggcaacaggatcaatg'3; Reverse: 5'ctgcagcttggagaagttcat'3), Col2a1 (Forward: 5'gccatcgccatagctgaa'3; Reverse: 5'cgactgtccctcggaaaa'3), ACAN (Forward: 5'ccagcctacaccccagtg'3; Reverse: 5'gagggtgggaagccatgt'3), *Runx2* (Forward: 5'gcccaggcgtatttcaga'3; Reverse: 5'tgcctggctcttcttactgag'3), Alp (Forward: 5'cggatcctgaccaaaaaacct'3; Reverse: 5'tcatgatgtccgtggtcaat'3), Col10 (Forward: 5'gcatctcccagcaccaga'3; Reverse: 5'ccatgaaccagggtcaagaa'3 ), were normalized against

Gapdh (Forward: 5'atgtgtccgttgtggatctg'3; Reverse: 5'ggtcctcagtgtagcccaag'3). CCM-treated VSC controls were used to reflect basal transcript levels. At each time point results were expressed as fold changes in transcript levels of the Il-6-treated cultures compared to CCM-treated VSC cultures. RNA integrity was assessed at all times and Supplementary Figure 10 shows a representative image of intact total RNA (RIN=10) obtained.

**Supplemental References**


1. da Silva Meirelles L, Chagastelles PC, Nardi NB. Mesenchymal stem cells reside in virtually all post-natal organs and tissues. **J Cell Sci**. 2006;119:2204-2213.
2. Sudres M, Norol F, Trenado A et al. Bone marrow mesenchymal stem cells suppress lymphocyte proliferation in vitro but fail to prevent graft-versus-host disease in mice. **J Immunol**. 2006;176:7761-7767.
3. Seluanov A, Vaidya A, Gorbunova V. Establishing primary adult fibroblast cultures from rodents. **J Vis Exp**. 2010.
4. Farrell E, O'Brien FJ, Doyle P et al. A collagen-glycosaminoglycan scaffold supports adult rat mesenchymal stem cell differentiation along osteogenic and chondrogenic routes. **Tissue engineering**. 2006;12:459-468.
5. Parhami F, Basseri B, Hwang J et al. High-density lipoprotein regulates calcification of vascular cells. **Circulation research**. 2002;91:570-576.
6. Lacey DC, Simmons PJ, Graves SE et al. Proinflammatory cytokines inhibit osteogenic differentiation from stem cells: implications for bone repair during inflammation. **Osteoarthritis Cartilage**. 2009;17:735-742.

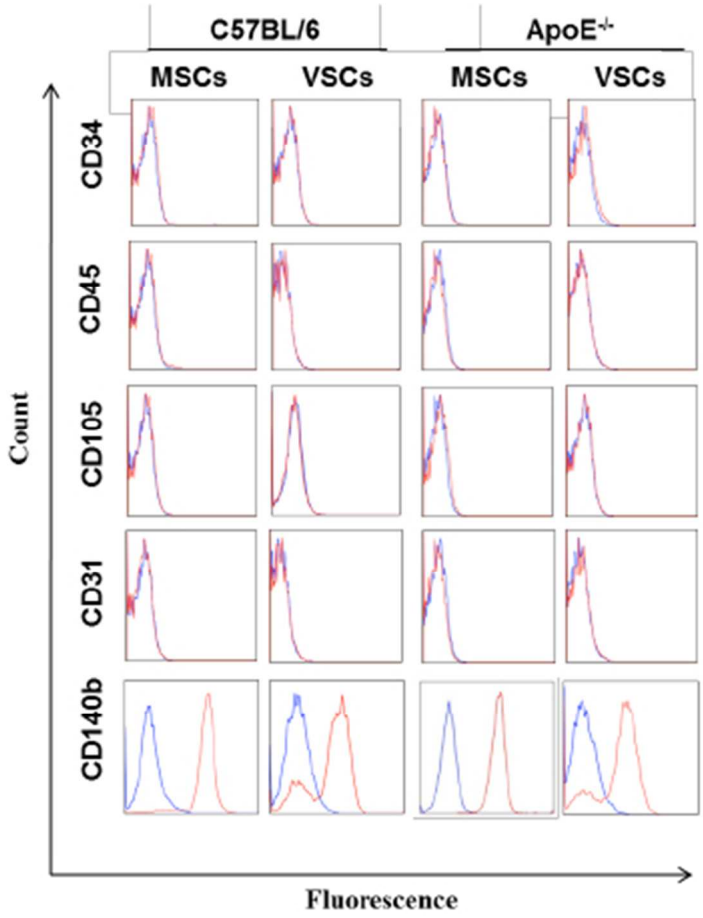


Supplementary Figure 1. Cell surface phenotype of VSCs and MSCs. The cells were phenotyped using flow cytometry for the negative MSCs markers, CD34, CD45, CD105, CD31 and the perivascular cell marker CD140b. Representative staining of MSCs and VSCs from C57BL/6 and ApoE-/- mice are displayed as histograms (red line- surface antigens and blue line- negative controls ).
30x41mm (300 x 300 DPI)

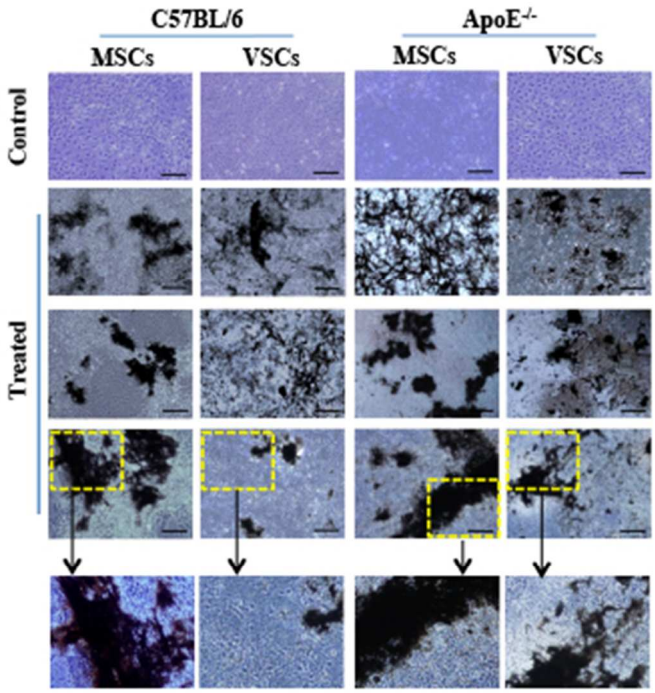


Supplementary Figure 2. Mineralization potential of isolated preparations. Representative Von Kossa staining of C57BL/6 and ApoE-/- MSCs and VSCs 14 days post-osteogenic induction. Cells cultured in control medium were negative; Scale bar, 500μm.
29x36mm (300 x 300 DPI)

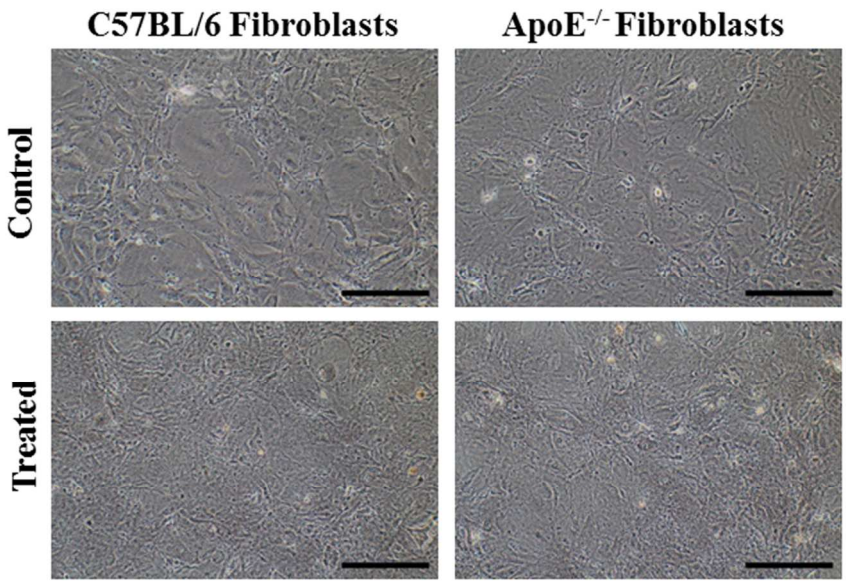


Supplementary Figure 3. Osteogenic potential of lung fibroblasts from C57BL/6 and ApoE-/- mice. Lung fibroblasts from either strain did not undergo osteogenic differentiation as visualized by lack of Von Kossa staining at day 14 post induction of osteogenesis. Scale bar, 200μm.
122x89mm (300 x 300 DPI)

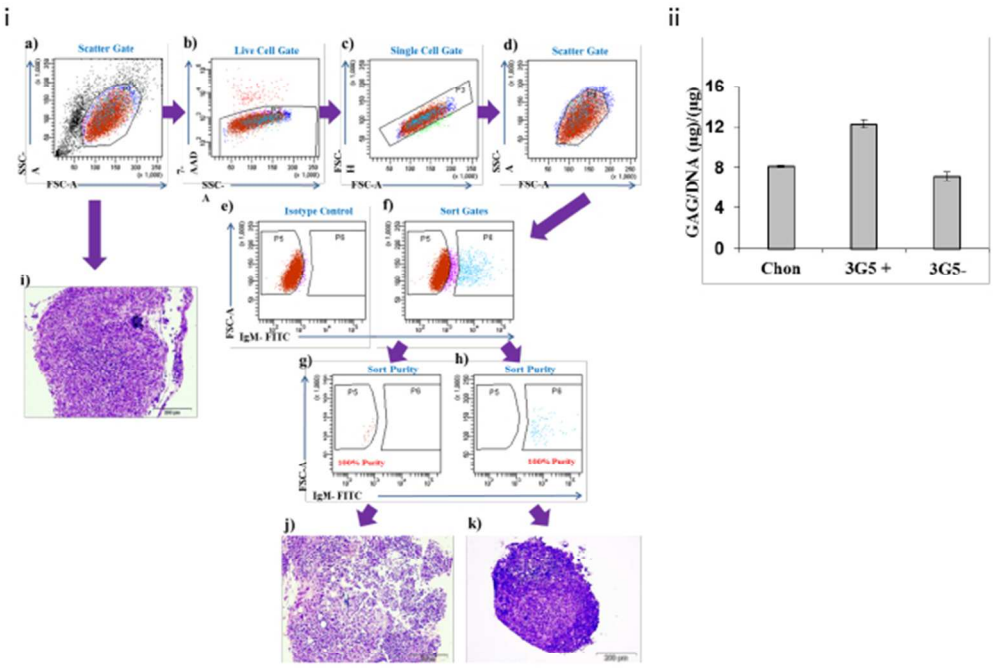


Supplementary Figure 4. Isolated VSCs were sorted by flow cytometry for expression of 3G5 and cell populations were characterized for chondrogenic differentiation. i) Viable cells were selected by the forward versus side scatter profile (a), with dead cells excluded by gating using 7-AAD (b), doublets by the single cell gate (c) and debris by the scatter gate (d). The isotype control and 3G5 sort gates are shown in e) and f), respectively where p5 is negative and p6 positive. Purity of each population was shown to be g) 100% negative and h) 100% positive. Sorted positive and negative 3G5 cells were subjected to chondrogenic assays. Parent VSCs (i) showed chondrogenic morphology whereas the negative fraction (j) did not form a defined pellet and the 3G5+ sorted cells (k) formed a hypertrophic pellet. Scale bar, 200μm. ii) 3G5+ cell fraction also had higher a GAG/DNA ratio compared to parent ApoE-/- VSCs and 3G5- sorted cells (n= 3 technical replicates).
57x43mm (300 x 300 DPI)

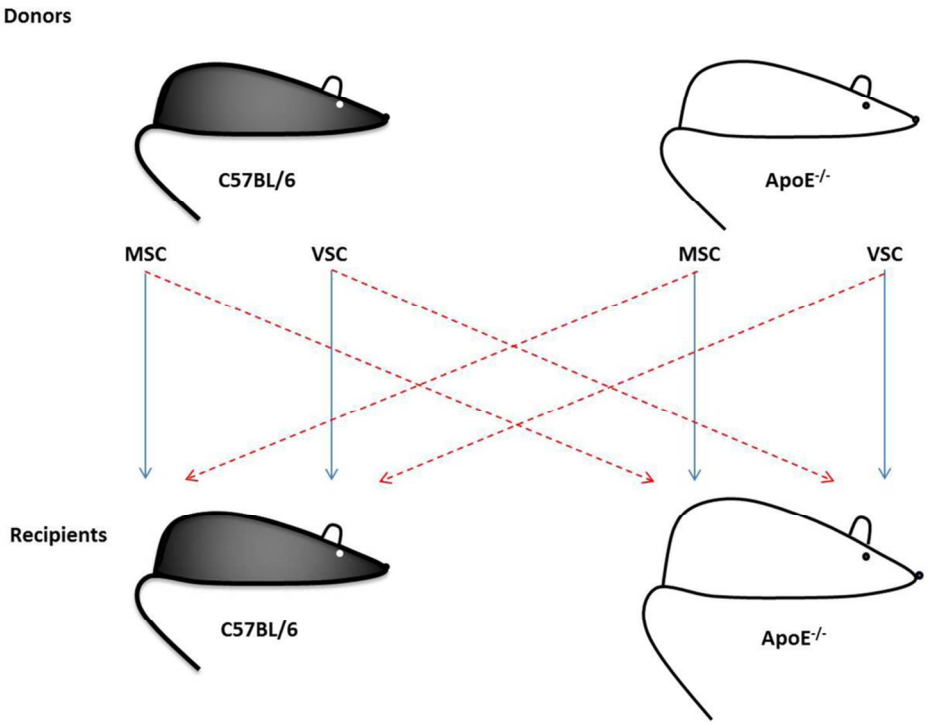


Supplementary Figure 5. Experimental design. Control, unprimed or chondrogenically-primed ApoE-/- and C57BL/6 MSCs and VSCs constructs were implanted subcutaneously in the back of C57BL/6 and ApoE-/- mice.
95x70mm (300 x 300 DPI)

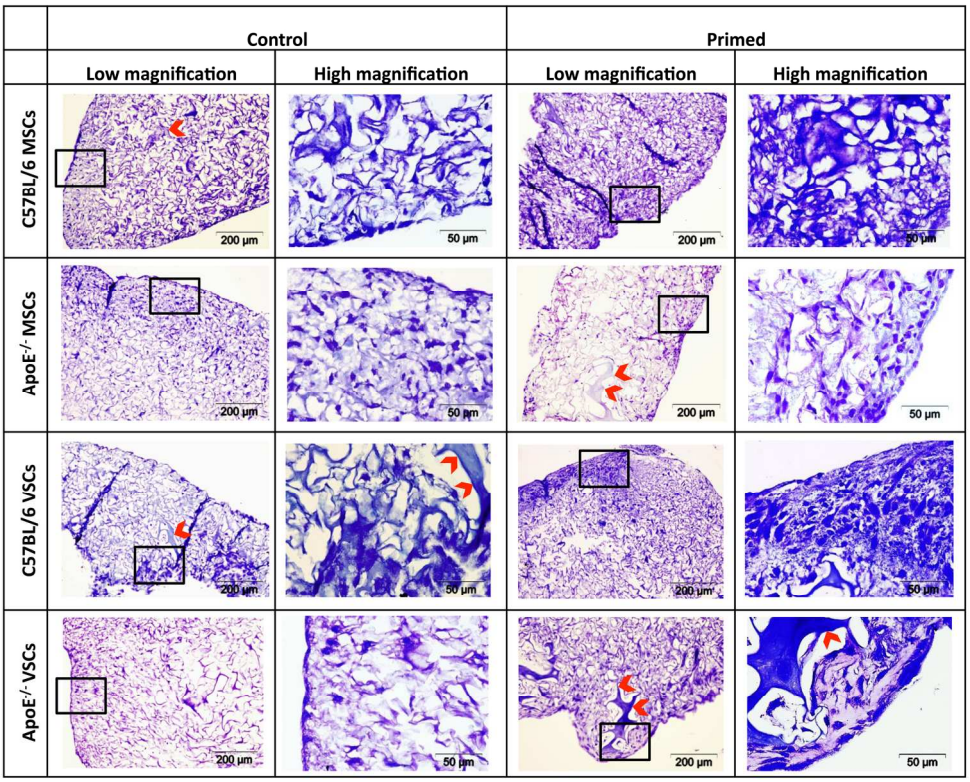


Supplementary Figure 6. Assessment of collagen-glycosaminoglycan scaffolds prior to in vivo implantation. Toluidine Blue staining showing homogenous cell distribution in both control and chondrogenically-primed constructs after 32 days in culture (Low and high magnification, 200µm and 50µm; red arrowheads, scaffold).
173x140mm (300 x 300 DPI)

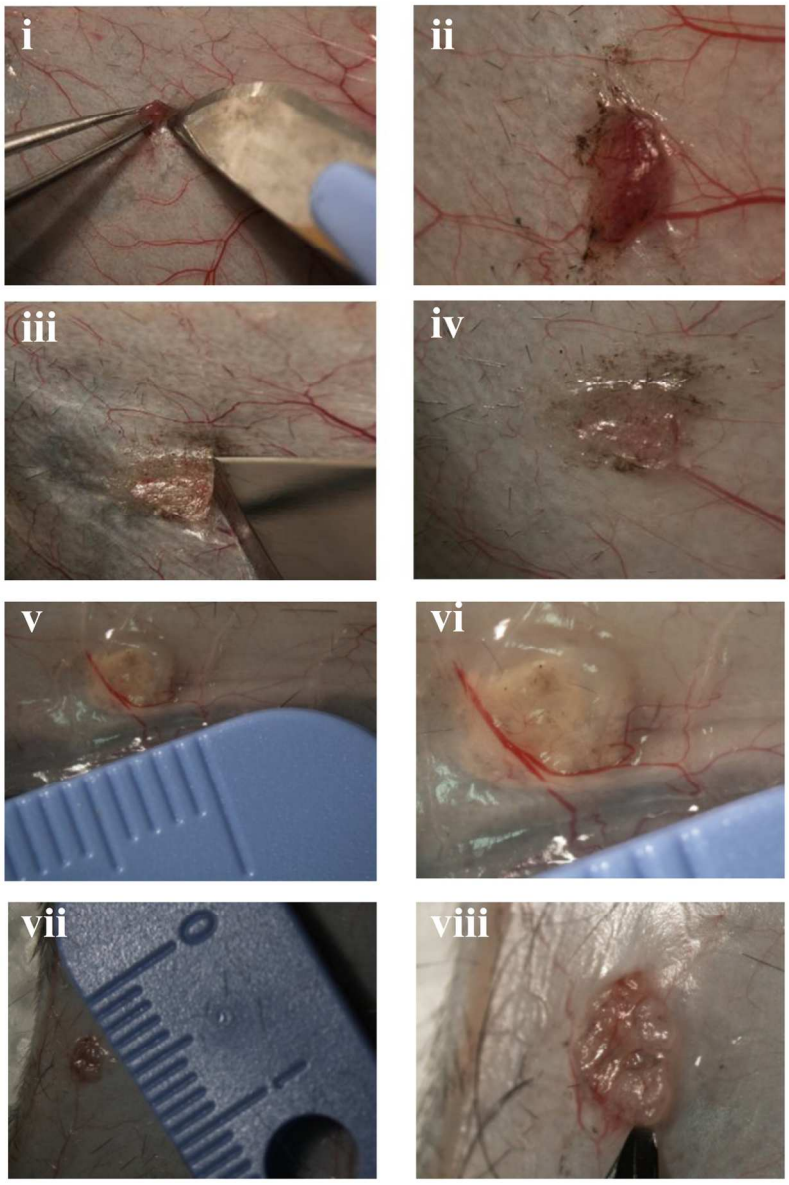


Supplementary Figure 7. Gross appearance of retrieved samples. After 8 weeks implantation, the level of bone formation, bone marrow as well as blood vessels and fat appearance in the retrieved constructs was analysed. Grossly, (i), (ii) chondrogenically primed ApoE-/- MSC constructs retrieved from C57BL/6 mice appeared vascularized. (iii), (iv) chondrogenically primed ApoE-/- MSC constructs retrieved from ApoE-/- mice had the appearance of hard bone-like structures. (v), (vi) chondrogenically primed ApoE-/- VSC constructs retrieved from C57BL/6 mice. (vii), (viii) chondrogenically primed ApoE-/- VSC constructs retrieved from ApoE-/- mice. These retrieved constructs seemed to have the appearance of hard bone-like structures and exhibited vascularization. Scale, 1 division - 1mm.
114x172mm (300 x 300 DPI)

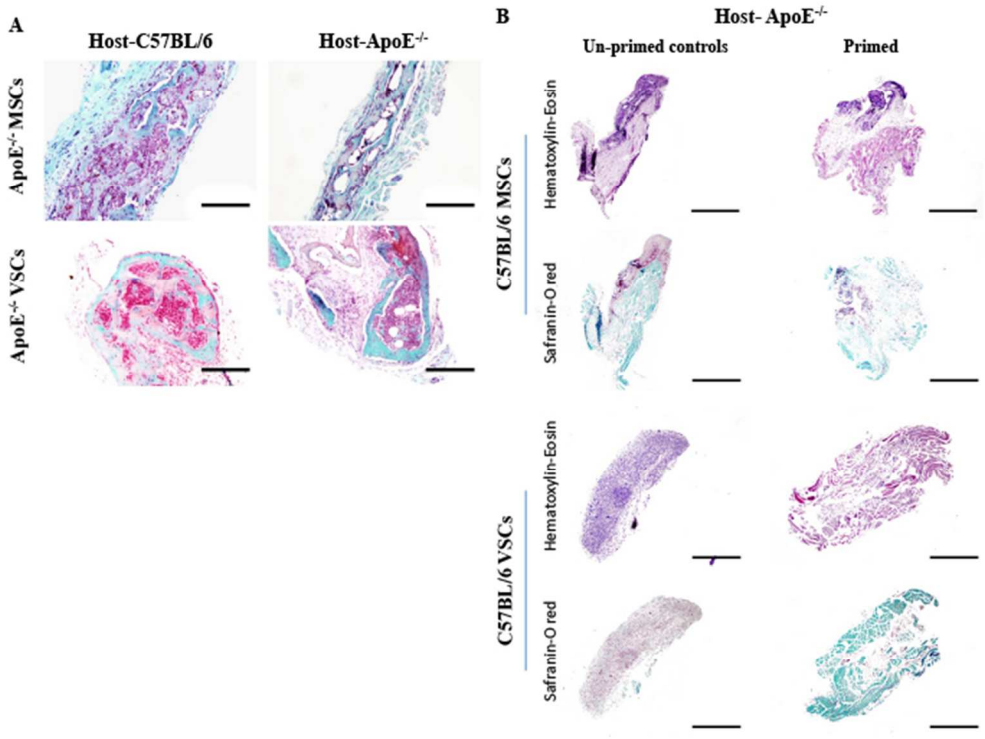


Supplementary Figure 8. Histologic and immunohistochemical characterization of retrieved constructs from C57BL/6 and ApoE-/-from primed and unprimed MSCs and VSCs. A, Representative Safranin-O red staining of primed ApoE-/- MSC and VSC constructs retrieved from ApoE-/- mice showing mature bone formation with well-developed bone marrow. Scale bars, 200μm. B, Histological examination of un-primed and primed C57BL/6 constructs retrieved from ApoE-/- mice. H&E and Safranin-O red staining were used to analyze matrix synthesis and GAG deposition, respectively.
58x44mm (300 x 300 DPI)

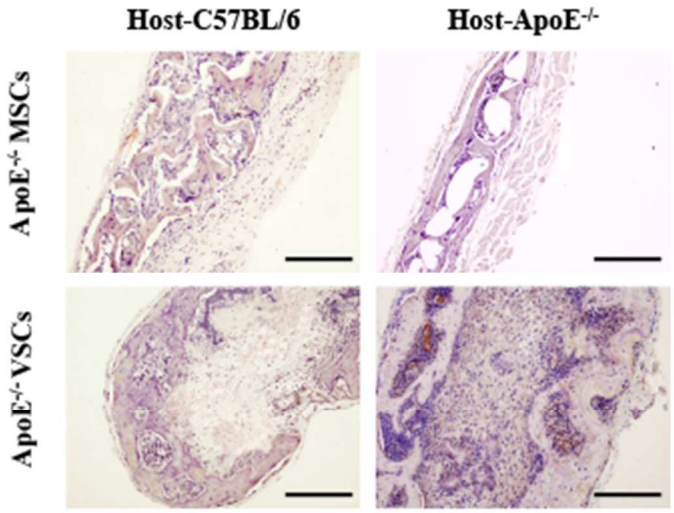


Supplementary Figure 9. Bone and matrix formation in primed ApoE-/- MSC and VSC constructs retrieved from C57BL/6 and ApoE-/- mice by type X collagen staining. Positive immunohistochemical localization of type X collagen, a marker of chondrocyte hypertrophy, is evident in the chondral portion of the constructs (Scale bars, 200μm).
28x23mm (300 x 300 DPI)

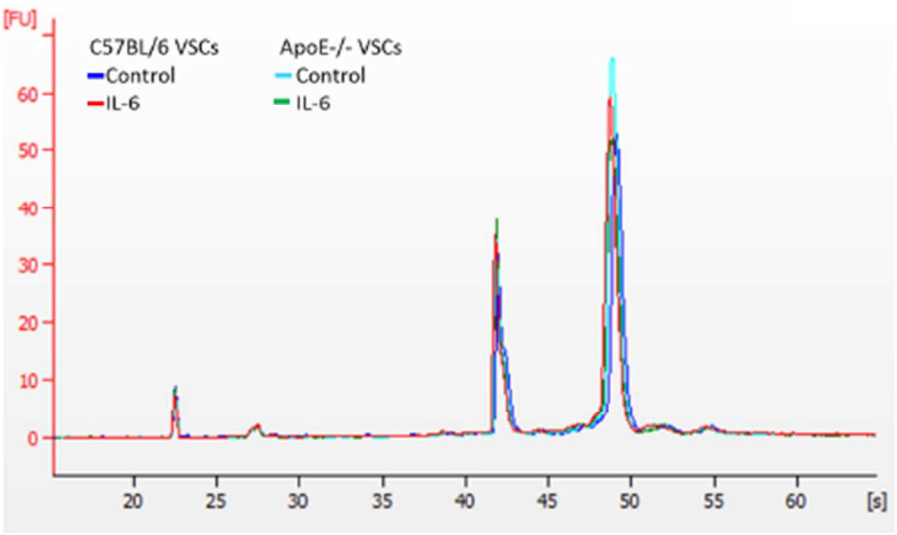


Supplementary Figure 10. Electropherograms (Agilent Bioanalyzer) from control and treated samples showing total RNA integrity. All scans show high quality and intact total RNA with RIN (RNA Integrity Number) equal to 10.
37x25mm (300 x 300 DPI)

**Supplementary Table 1. Growth profile of cell populations.** Doubling time (days) was calculated from three independent isolations for all cell preparations using data from the passages (P) indicated.

| | **MSCs** | **VSCs** |
|---|---|---|
| **ApoE$^{-/-}$** | 1.5, 1.5, 1.3 (P6-14) | 1.8, 1.5, 1.6 (P6-14) |
| **C57BL/6** | 2.7, 2.3, 2.7 (P7-14) | 1.7, 1.8, 1.8 (P6-14) |

**Supplementary Table 2. Surface characteristic of isolated cells by flow cytometry.** Values are presented as the mean ±SD of 3 preparations and represent percentage positive cells

| | C57BL/6 | | ApoE $^{-/-}$ | |
|---|---|---|---|---|
| **Surface marker expression** | **MSCs** | **VSCs** | **MSCs** | **VSCs** |
| MSC associated antigens | | | | |
| Sca-1 | 86.5±4.84 | 91.73±4.12 | 91.46±1.7 | 95.16±2.8 |
| CD44 | 59.05±1.34 | 70.2±11.59 | 66.26±2.05 | 77.93±9.71 |
| CD90.2 | 16.6±2.26 | 97.86±2.23 | 6.54±0.13 | 81.35±0.91 |
| Pericyte associated antigens | | | | |
| 3G5 | 0.72±0.92 | 9.29±2.14 | 1.44±0.34 | 41±1.43 |
| Tie-2 | 1.02±0.43 | 0.57±0.83 | 0.28±0.37 | 0.54±0.31 |
| CD146 | 2.29±2.25 | 43.66±5.51 | 1.03±1.4 | 47.6±3.41 |
| CD140b | 92.7±3.2 | 57.2±5.4 | 97.6±1.4 | 70.2±5.8 |
| Hematopoietic associated antigens | | | | |
| CD34 | 0.111±0.08 | 2.57±1.38 | 1.68±0.97 | 1.76±0.90 |
| CD45 | 0.099±0.12 | 0.78±0.72 | 1.1±0.42 | 0.973±1.23 |
| CD105 | 0.21±0.27 | 4.95±3.28 | 1.04±0.21 | 4.4±4.9 |
| Endothelial associated antigens | | | | |
| CD31 | 0.09±0.12 | 0.89±0.80 | 0.76±0.17 | 1.02±1.24 |

**Supplementary Table 3. Histological grading scale for subcutaneous retrieved samples** The grading score took in to account the appearance of bone, cartilage, bone marrow, fat, fibrous matrix and blood vessel formation as well as surrounding host tissue.

| Percent volume (%) of the total retrieved sample | Score |
|---|---|
| 76-100% | 4 |
| 51-75% | 3 |
| 26-50% | 2 |
| 1-25% | 1 |
| 0% | 0 |